SPACE RESEARCH COORDINATION CENTER

MECHANICAL PROPERTIES OF THE GROUP IVB AND VB TRANSITION METAL MONOCARBIDES

BY

W.F. BRIZES

DEPARTMENT OF METALLURGICAL AND MATERIALS ENGINEERING

SRCC REPORT NO. 80

UNIVERSITY OF PITTSBURGH

PITTSBURGH, PENNSYLVANIA

11 JULY 1968

The Space Research Coordination Center, established in May, 1963, has the following functions: (1) it administers predoctoral and postdoctoral fellowships in space-related science and engineering programs; (2) it makes available, on application and after review, allocations to assist new faculty members in the Division of the Natural Sciences and the School of Engineering to initiate research programs or to permit established faculty members to do preliminary work on research ideas of a novel character; (3) in the Division of the Natural Sciences it makes an annual allocation of funds to the interdisciplinary Laboratory for Atmospheric and Space Sciences; (4) in the School of Engineering it makes a similar allocation of funds to the Department of Metallurgical and Materials Engineering and to the program in Engineering Systems Management of the Department of Industrial Engineering; and (5) in concert with the University's Knowledge Availability Systems Center, it seeks to assist in the orderly transfer of new space-generated knowledge in industrial application. The Center also issues periodic reports of space-oriented research and a comprehensive annual report.

The Center is supported by an Institutional Grant (NsG-416) from the National Aeronautics and Space Administration, strongly supplemented by grants from the A. W. Mellon Educational and Charitable Trust, the Maurice Falk Medical Fund, the Richard King Mellon Foundation and the Sarah Mellon Scaife Foundation. Much of the work described in SRCC reports is financed by other grants, made to individual faculty members.

ABSTRACT

The mechanical behavior of the Group IVB and Group VB monocarbides have been studied on one hundred percent dense samples made by liquid state carburization. The properties investigated were thermal expansion, yield stress, and room temperature hardness as a function of stoichiometry. The activation energy for deformation of niobium carbide was determined from high temperature yield stress data and was found to be 133K cal/mole, a value that is in good agreement with the estimated activation energy for niobium diffusion in niobium monocarbide.

TABLE OF CONTENTS

LIST OF FIGURES

LIST OF FIGURES (CONTINUED)

LIST OF TABLES

1.0 INTRODUCTION

The carbides of the Group IVB and VB transition elements are of special interest in the field of high temperature technology because of their high melting points and structural capabilities at temperatures above 2000°C. They are of special interest for use in nuclear rocket applications where most conventional structural materials would be molten. However, the advantage of the high temperature strength is somewhat offset by the fact that the carbides have a brittle to ductile transition temperature above 1000°C.

The structure of the transition metal monocarbides are B_1, i. e., having a sodium chloride type arrangement where the carbon and metal atoms exist in two inter-penetrating face-centered cubic lattices. The carbide structure is quite stable relative to carbon composition and can exist over a wide range of compositions. In the carbide the metal atom sites are considered to be filled while the carbon atom sites may be depleted by as much as fifty percent. The carbon-metal phase diagrams for the six transition elements are given in Figures 1 through 6.

The electronic structure of titanium carbide has been studied by light reflectivity[11], photoemission[11], the Hall coefficient[12] [13], and resistivity[12]. It is believed[14] that the prominent bonding in titanium carbide is due to strong covalent metal-metal interactions. The interactions in the carbide are,however, greater than in the parent metal due to the reinforcement of the metal-metal bonds by carbon in the region of overlap between metal orbitals and because the electrons participating in such bonding are increased by transfer of electrons from carbon to metal atomic orbitals[14]. Metal-carbon and carbon-carbon interaction are also thought to be important.

The slip system in titanium carbide has been identified by etch pit[15] and electron microscopy[16] studies to be $\{111\}\langle 1\bar{1}0\rangle$. This deformation system is also assumed for the other five monocarbides namely ZrC, HFC, TaC, NbC and VC.

The purpose of the present study was to investigate the high temperature mechanical behavior of the six Group IVB and VB monocarbides simultaneously so that their relative behavior might be related to such properties as: Peierls force, thermal expansion, melting point and diffusivity. This study would then provide the foundation for investigating the behavior of alloy carbides.

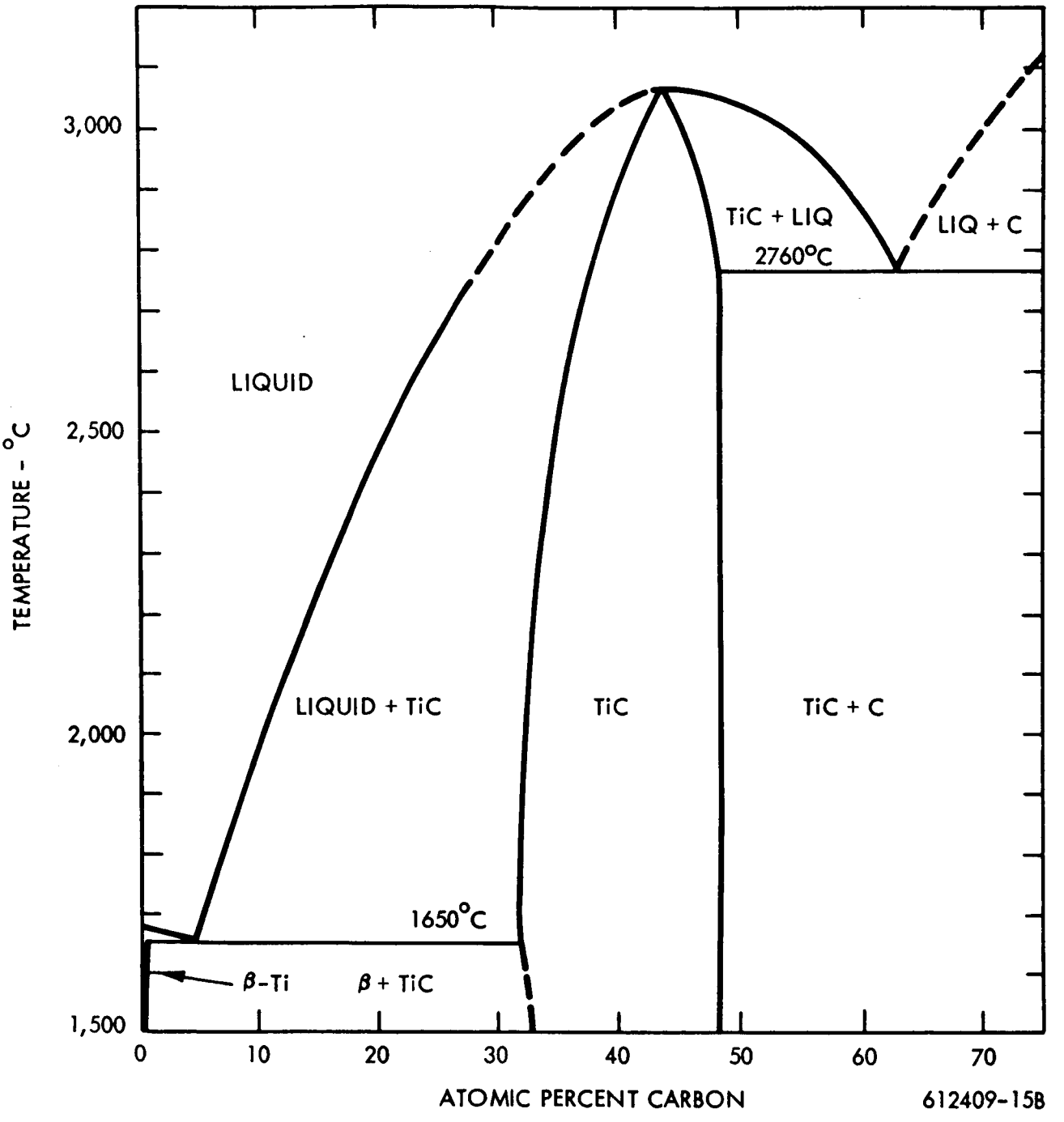

Figure 1. Titanium - Carbon Phase Diagram[1] [2]

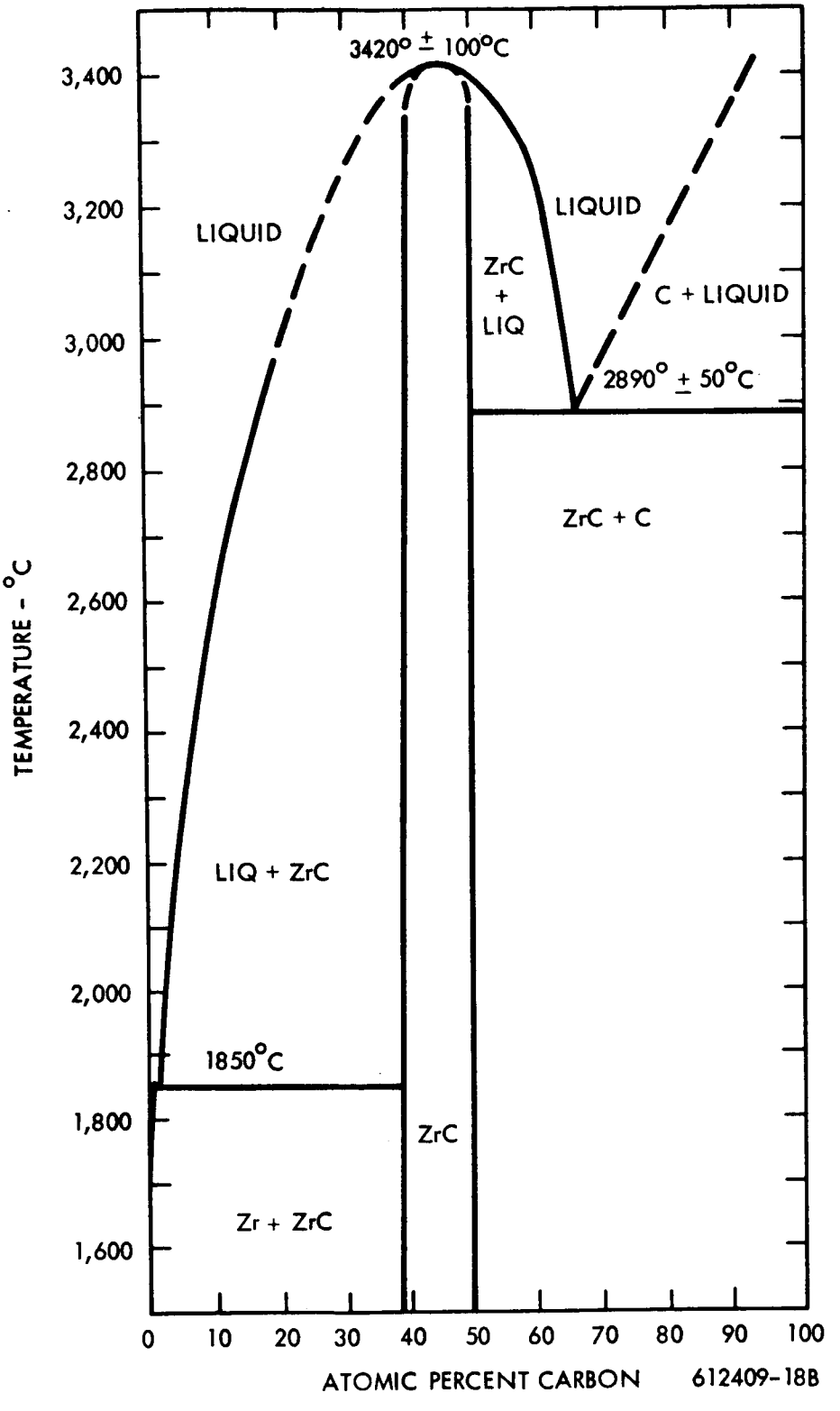

Figure 2. Zirconium - Carbon Phase Diagram[3] [4]

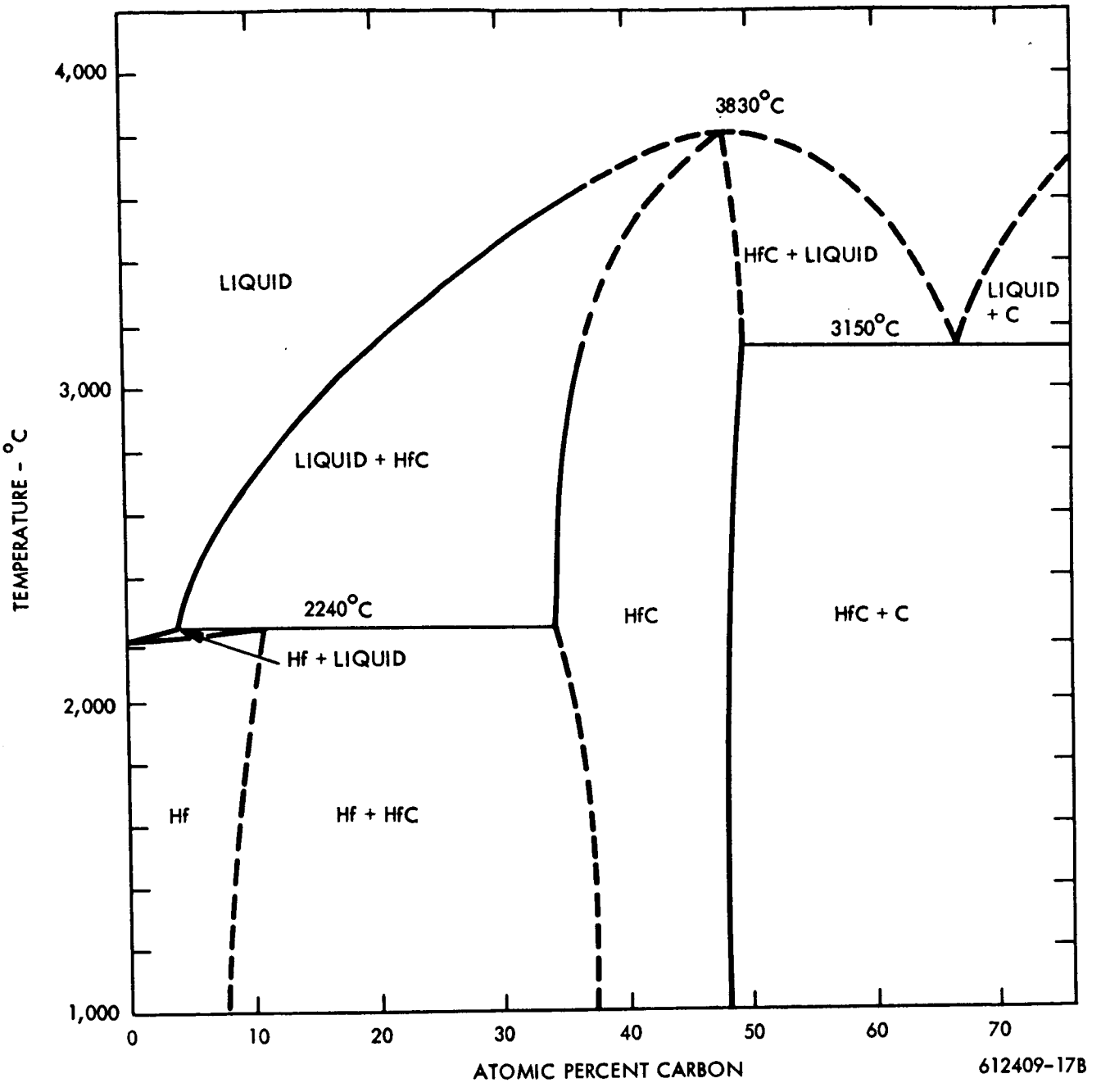

Figure 3. Hafnium - Carbon Phase Diagram[1] [5]

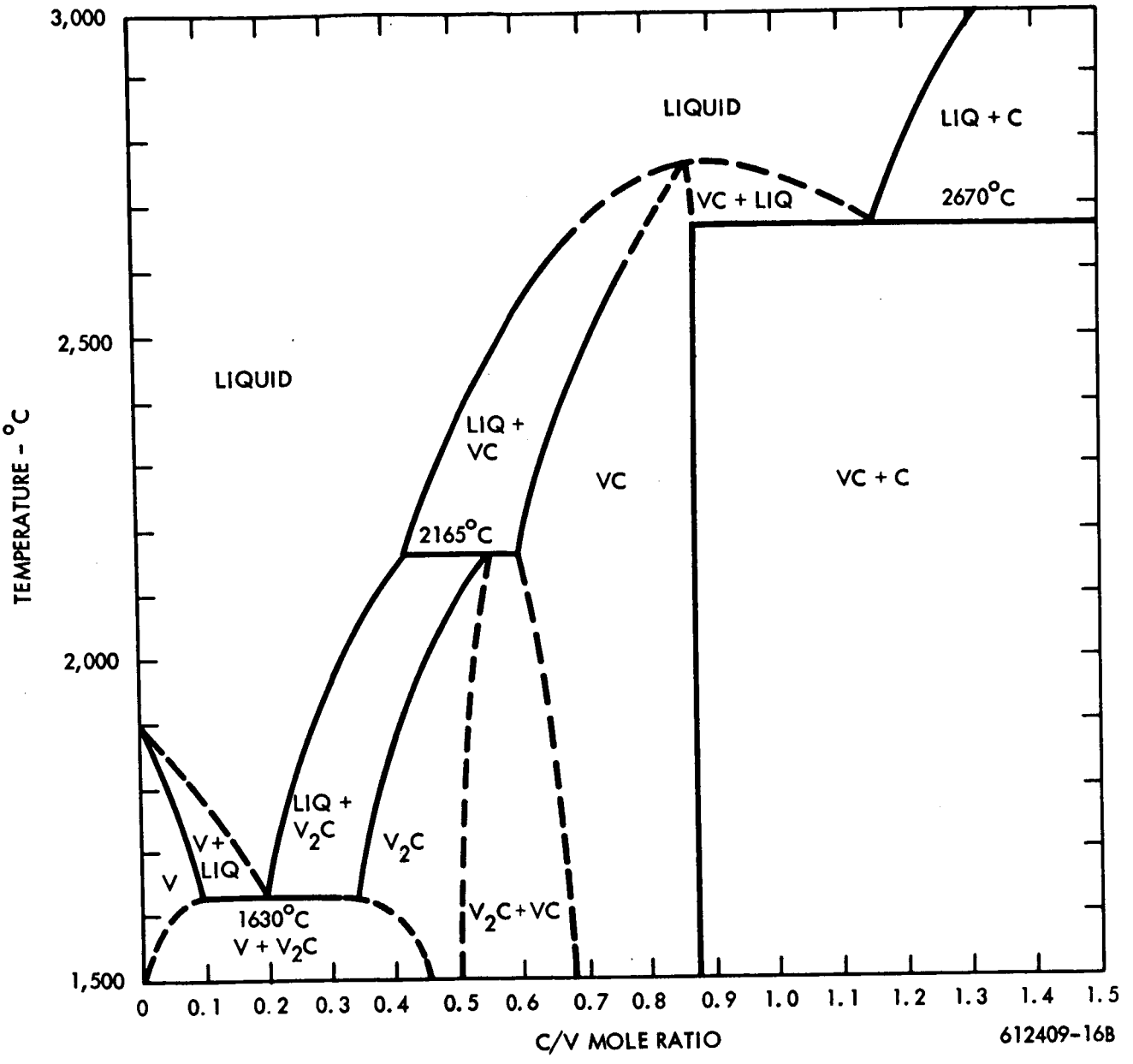

Figure 4. Vanadium - Carbon Phase Diagram[6] [7]

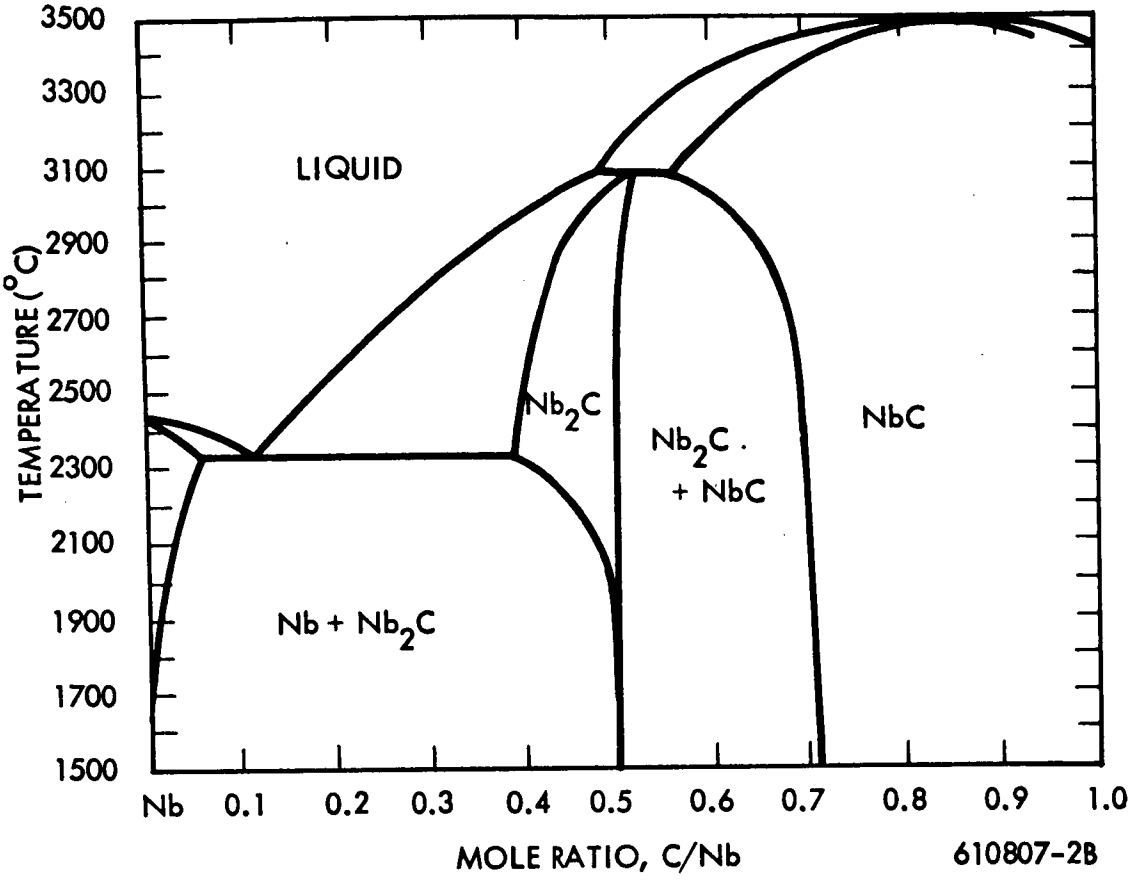

Figure 5. Niobium - Carbon Phase Diagram[8]

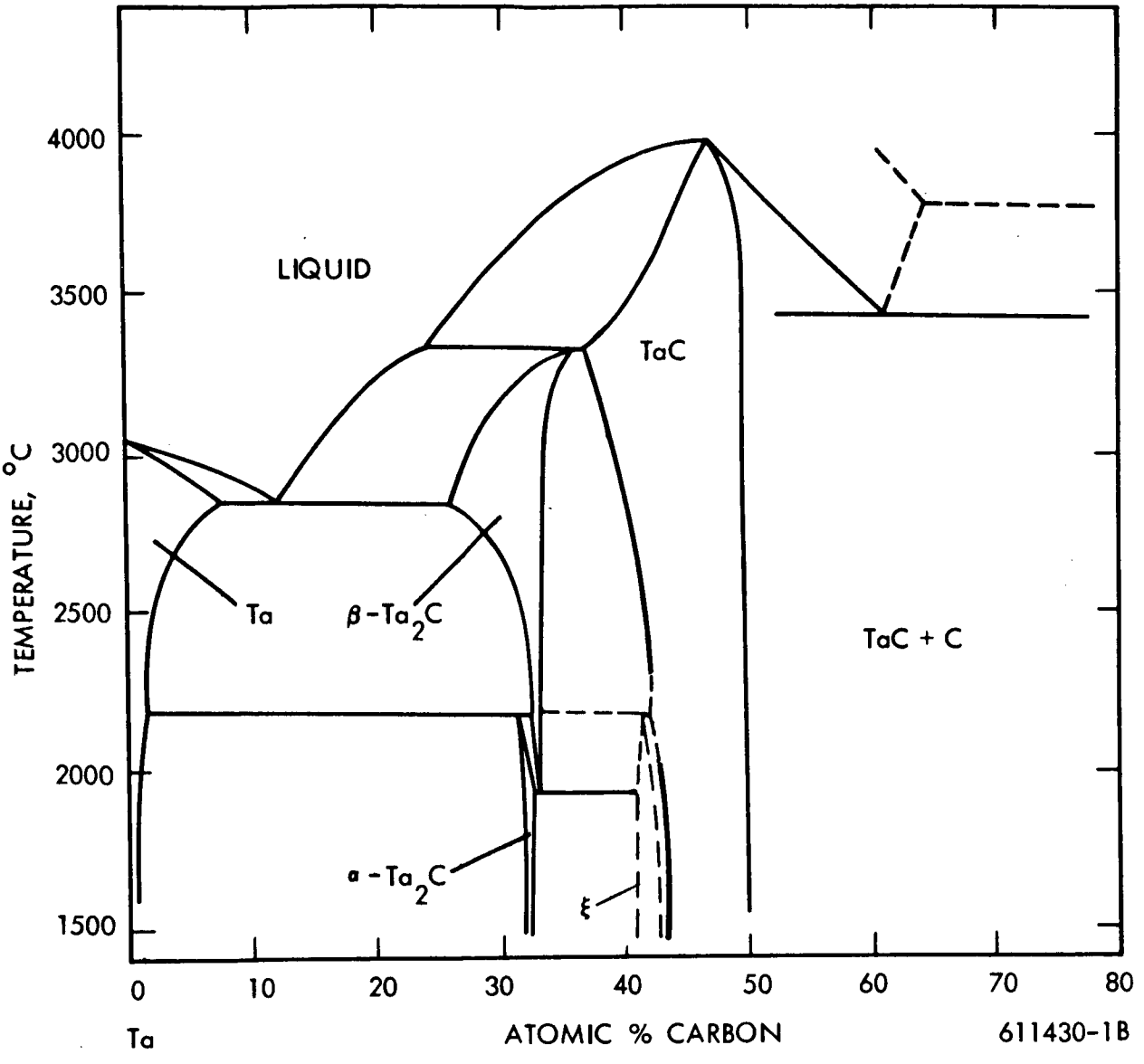

Figure 6. Tantalum - Carbon Phase Diagram[9] [10]

2.0 SPECIMEN PREPARATION

Transition metal carbide test specimens have been made by 1) cold pressing and sintering, 2) hot pressing, 3) the Verneuil technique, 4) zone melting, 5) solid state carburization and 6) liquid state carburization. The first four methods usually involve starting with a fine powder and thus are susceptible to high impurity contents. Cold pressing followed by sintering and hot pressing techniques normally produce a carbide containing porosity. It has been shown by Ryshkewitch[17] that a small amount of porosity in a ceramic has a major effect on strength;for example, ten percent porosity in Al_2O_3 reduces the strength by one-half. Thus, specimens containing porosity are not completely satisfactory for measuring deformation properties of the carbides. Solid state carburization appears novel in that complex carbide shapes can be made from premachined metal shapes;however,diffusion annealing times are long for sample shapes other than wire or thin sheet configurations. Also the specimen usually contains surface cracks resulting from the volume expansion of the carbide as it is formed from the metal. Liquid state carburization has the benefit of low impurity content since crystal bar or electron beam processed metal can be melted directly. Surface cracks observed in solid state carburization do not occur since the annealing temperature is high enough for stresses in the carbide to be relieved by plastic flow. Thus the liquid state carburization method was chosen for fabrication of the six transition metal carbides studied. The specimens were made by inserting high purity metal rods into graphite molds and diffusion annealing for one to two weeks at approximately 200°C below the carbide-carbon eutectic temperature (see Figures 1 through 6). The carburization was done in a modified high temperature graphite furnace previously described[3]. The resulting rods (six rods 3/8 inch dia. by 3 inches long) were coarse grain, i. e., two to three grains across the diameter except for hafnium carbide which contained approximately ten grains across the diameter. The rods were then cut into compression specimens (3/8 inch diameter by 3/4 inch long) using a diamond wheel. Since the specimens were made in a carbonaceous atmosphere, they were of the highest carbon content attainable predicted by the phase diagram. The carbon analysis after mechanical testing is given in

Table 1 together with the lattice parameters. Chemical and spectrographic analysis of the specimens after testing are given in Table 2. An electron micrograph of zirconium carbide showing the low dislocation density of the as-grown carbide is shown in Figure 7.

TABLE 1

CARBON AND X-RAY ANALYSIS AFTER TESTING

	Wt % Carbon	Atomic % Carbon	$\frac{C}{Me}$	a_o (Å)
TiC	19.39	49.0	0.961	4.3259
ZrC	11.53	49.7	0.99	4.6981
HfC	6.24	50.0	1.00	4.6421
VC	17.10	46.7	0.876	4.1655
NbC	11.13	49.2	0.969	4.4691
TaC	6.27	50.2	1.00	4.4534

TABLE 2

CHEMICAL AND SPECTROGRAPHIC ANALYSIS AFTER TESTING, PPM

	TiC	ZrC	HfC	VC	NbC	TaC
O	743	25	11	13	9	7
N	<20	<20	<20	<20	<20	<20
H	1.5	2.5	0.6	1.6	1.0	1.3
Ag	< 3	18	22	< 2	< 3	< 3
Al	150	<10	<10	< 2	<10	<10
Au	<100	<300	<300	--	--	--
B	--	4.0	< 1	240	< 1	< 1
Ba	<10	< 10	< 3	< 6	< 3	<10
Be	< 3	< 0.3	< 0.3	< 0.6	< 0.3	< 0.3
Bi	<30	< 10	< 30	<60	<10	<100
Ca	<10	< 10	< 3	<60	<10	<10
Cd	<100	<100	<100	<600	<100	<300
Co	< 30	< 10	< 10	< 6	<30	<10
Cr	110	< 3	< 10	16	<10	<30
Cs	<100	<100	<100	<200	<100	<100
Cu	6.7	< 3	< 3	< 6	< 10	< 3
Fe	1000	93	< 30	1280	< 13	<10
Hf	--	96	--	--	--	--
In	<100	< 30	< 30	<60	< 30	<100
K	< 10	< 30	<10	<20	< 3	< 30
Li	< 3	< 3	< 1	< 6	< 1	< 3
Mg	13	< 1	< 3	<0.6	< 1	< 0.3
Mn	13	< 3	< 3	<0.6	< 3	< 1
Mo	< 30	18	22	160	<25	< 30
Na	< 3	<10	< 3	< 6	<10	< 10
Nb	200	< 30	<100	<600	--	< 30
Ni	27	< 3	< 10	51	<10	< 10
P	<300	<100	<100	<200	<100	<300
Pb	< 10	< 30	< 30	< 6	< 30	<100
Rb	< 30	<100	< 30	< 60	< 30	< 30
Sb	< 30	< 30	< 30	< 20	<100	<100
Si	110	< 10	< 10	160	< 10	< 3
Sn	40	<10	< 30	< 6	< 30	< 30
Sr	< 3	< 30	< 10	< 60	< 30	<100
Th	<100	< 30	<100	<600	<100	<100
Ti	--	15	33	19	10	< 10
Ta	--	<300	--	--	<300	--
U	<100	--	--	--	<300	<300
V	1200	< 3	< 3	--	< 10	< 10
W	<100	<100	< 30	<2000	<300	<300
Zn	<100	<100	<100	< 60	<100	<100
Zr	< 30	--	14500	<200	250	< 3

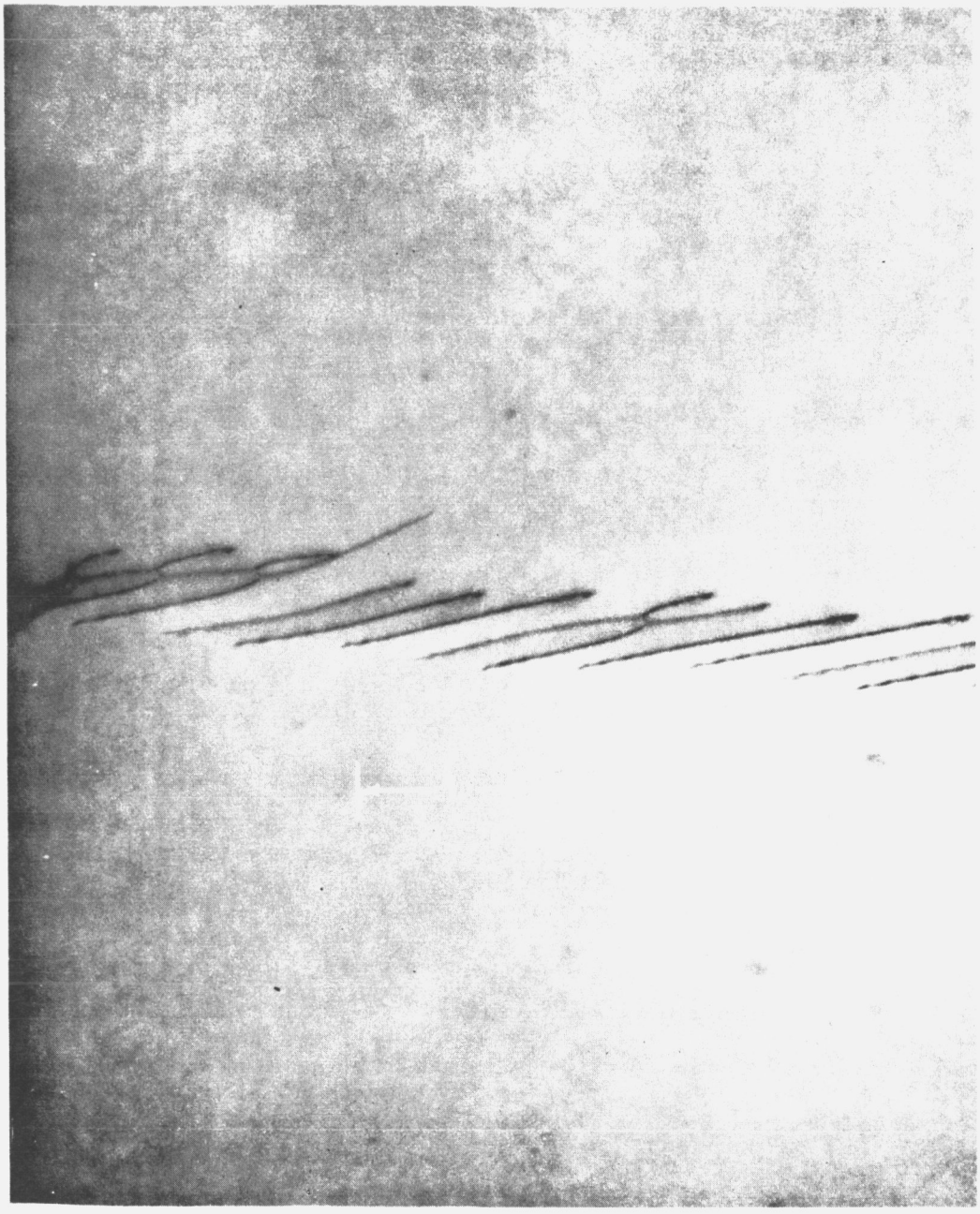

Figure 7. Electron Micrograph of a Sub-Boundary in As-Grown Zirconium Carbide

3.0 RESULTS

3.1 SUMMARY OF RESULTS

1) The thermal expansion within Group IVB and VB monocarbides appear to be inversely related to the melting points of the carbides.

2) The hardness of the Group IVB carbides decreases with decreasing carbon content while the Group VB carbides increased with decreasing carbon composition. A maximum in the hardness of tantalum monocarbide at low stoichiometry was obtained and the decrease in hardness at low stoichiometry was attributed to a precipitation phenomena.

3) At low temperatures the yield stress of all six monocarbides showed a strong temperature dependence and became temperature independent at temperatures greater than one-half the melting point.

4) At temperatures greater than one-half the melting point, the yield stress and creep resistance of tantalum carbide and titanium carbide were found to decrease with decreasing stoichiometry.

5) Gross grain boundary sliding was observed in both hafnium and vanadium carbide at elevated temperatures.

6) The activation energy derived from yield stress data for niobium carbide at a temperature greater than one-half the melting point agrees quite well with the estimated activation energy for metal diffusion in the carbide.

3.2 THERMAL EXPANSION

Thermal expansion measurements of five monocarbides were made on 1/4 inch diameter by 3 inch long specimens from 500 to 2050°C. Vanadium carbide was measured separately to a slightly higher temperature. The expansion measurements were carried out in a graphite resistance furnace containing all five specimens and a tungsten standard. The furnace was operated at a pressure of 15 microns (back filled with He) and utilizes two graphite hair-pin heating elements to obtain a uniform temperature zone. The specimens were mounted upright on a

pedestal between the two heating elements and were visible through viewing ports in the front and back of the furnace. Attached to the top and bottom of each specimen are sharp-edged graphite target flags that are easily distinguishable when viewed at a high temperature or with back lighting. The measuring device consists of two telescopes mounted in a frame anchored in a large surface stone that is free to traverse on an air-bearing surface from sample to sample across a larger granite stone that provides the stable platform necessary for accurate measurements. The telescopes are equipped with motor driven filar eyepieces and transmitting potentiometers. Low temperatures were measured with an infrared pyrometer and high temperatures with a Millitron two-color pyrometer. The overall accuracy of the system is estimated[18] to be $\pm$ 2 percent of the measured value at 2000°C and to have a temperature uniformity of $\pm$ 5°C.

The coefficient of thermal expansion as a function of temperature of the six monocarbides and tungsten is given in Figures 8 and 9. The expansion coefficient of tungsten extrapolated to room temperature is in excellent agreement with reported values [19]. The data for the carbides are in fair agreement with other investigators. A recent bibliography on thermal expansion of the carbides is given by Fries and Wahman [20].

It is interesting to note that the thermal expansion of the carbides do not reflect the increased bonding relative to the metal. At room temperature Young's Modulus [21] shows a significant change from about 20×10^6 psi to approximately 50×10^6 psi for the metal and carbide respectively. The coefficient of expansion for the pure metals is also given in Figures 8 and 9 and is approximately equal to the coefficient of expansion of the carbides when extrapolated to room temperature. There does, however, appear to be a relationship between the melting points of the carbides within each Group and the coefficient of thermal expansion such that alpha decreases with increasing melting temperature as shown in Figures 8 and 9.

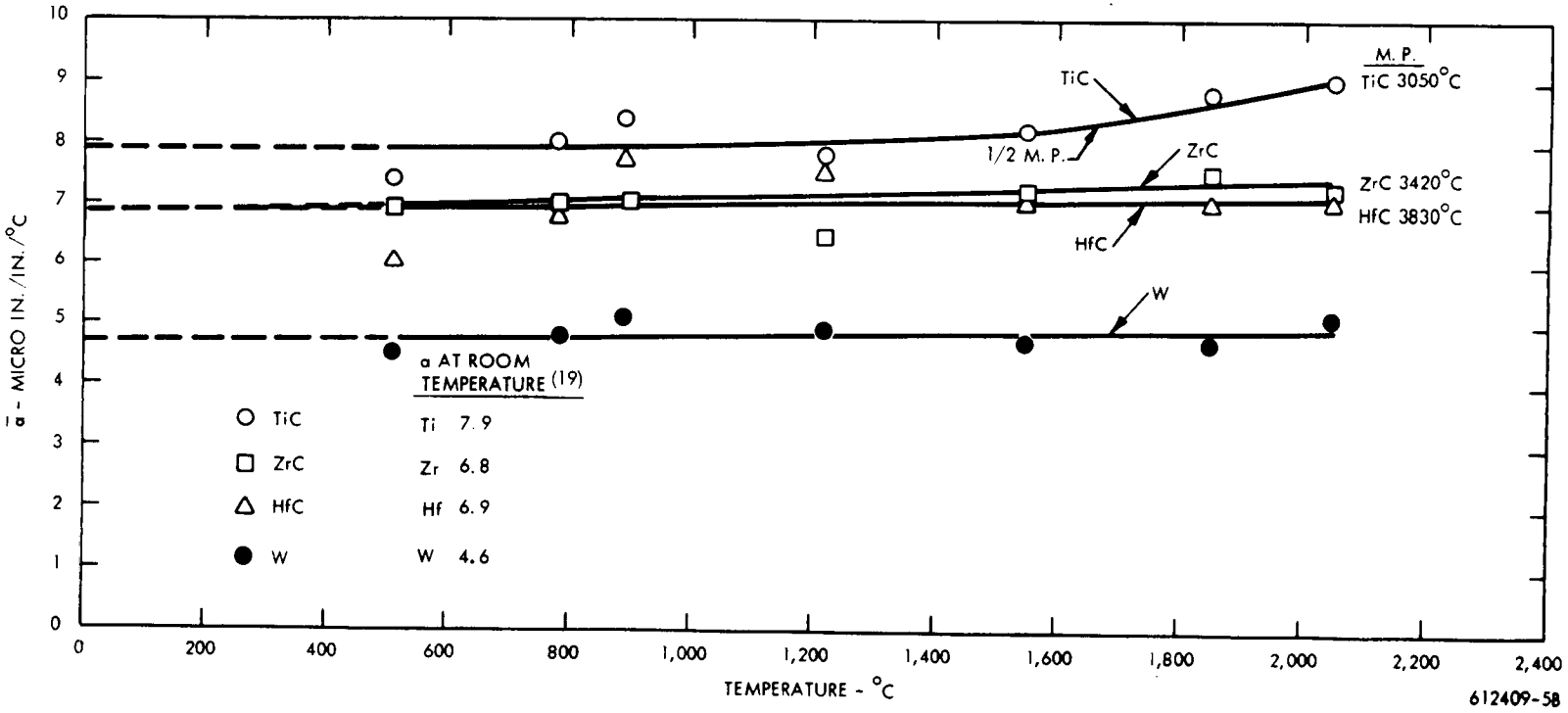

Figure 8. Coefficient of Thermal Expansion, $\bar{a}$, for the Group IVB Carbides as a Function of Temperature

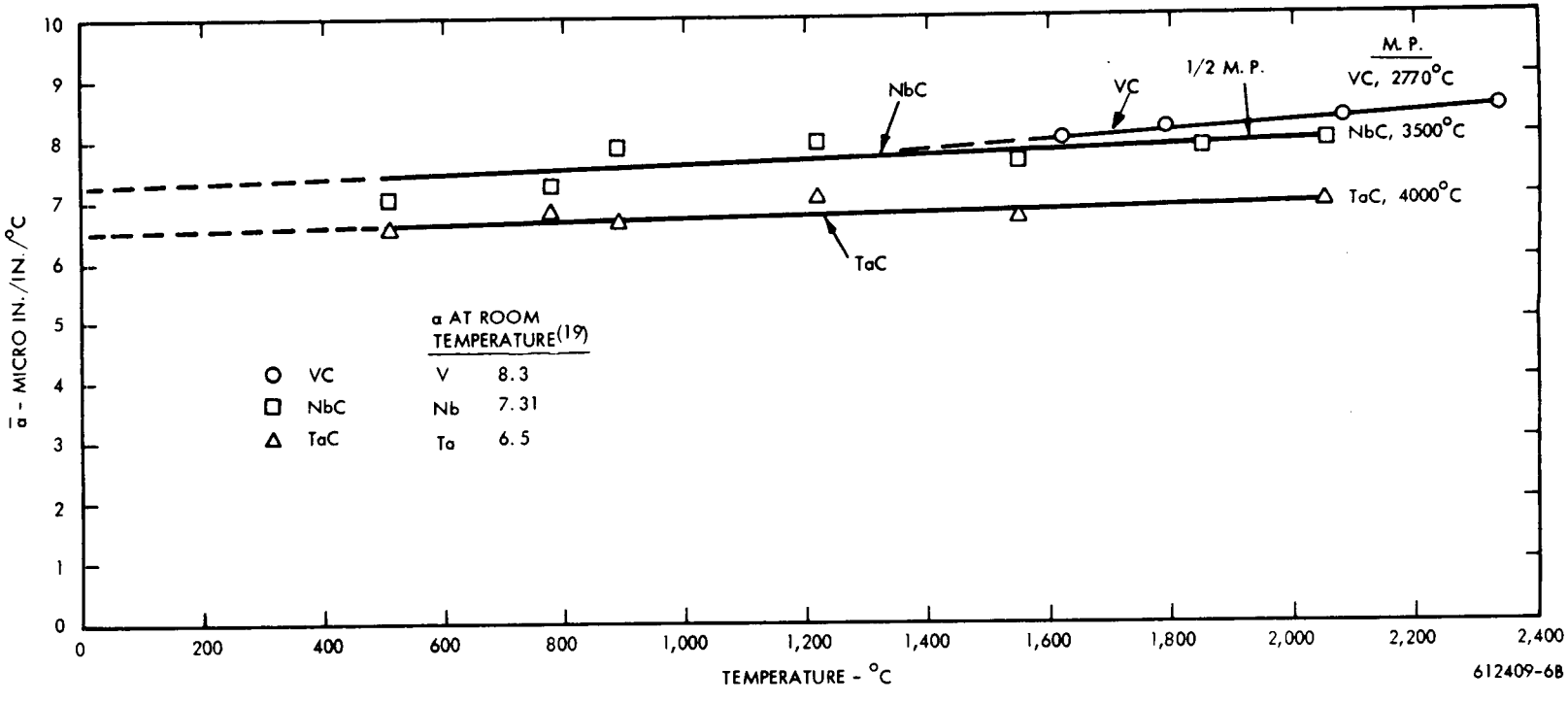

Figure 9. Coefficient of Thermal Expansion, $\bar{\alpha}$, for the Group VB Monocarbides as a Function of Temperature

3.3 HARDNESS

The room temperature hardness of the transition metal carbides has been measured by many investigators. Reviews of the hardness data have been given by Schwarzkopf and Kieffer[22] and by Samsonov and Umanskiy[23]. It is generally agreed that the Group IVB carbides are harder than the Group VB and that titanium carbide and tantalum carbide have the highest and lowest hardness, respectively.

The object of the present study was not to redetermine the hardness of high stoichiometry monocarbides but rather to determine the variation in hardness as a function of stoichiometry. Samples were prepared by reacting liquid metal and graphite until a sizeable carbide layer was formed. The carbide layer thus contained the entire range of carbon composition predicted by the phase diagram. Microhardness measurements were made in a single grain across the entire layer. This was done to eliminate orientation effects since the hardness is known to vary with orientation[24]. The hardnesses of the Group IV and V monocarbides across the carbide scale are given in Figures 10 and 11. It is evident that as carbon is removed from the Group IV carbides the hardness decreases. The opposite effect,however,is observed in the Group V carbides. The decrease of hardness and yield strength with decreasing stoichiometry has been observed by Williams and Lye[24] for TiC and is attributed to the removal of electrons associated with carbon atoms from the metal-metal bonds. If the same reasoning can be applied to the Group V carbides, it appears that they have an excess electron to atom ratio and by reducing the carbon content the strength therefore increases. It follows that if the Group IV has a deficient electron to atom ratio and the Group V has an excess then alloying[25] the two Groups should produce an optimum in the bonding. Recent work[25] on alloys of niobium-hafnium and niobium-zirconium carbides have shown a hardness peak at approximately 50 atomic percent niobium. Alloys of niobium-tantalum and hafnium-zirconium carbides did not show a peak as expected since these alloys were within the same Group. Work of Janng et al.[26] has shown a hardness peak in the systems TiC-VC and in HfC-TaC.

The hardness of tantalum carbide as a function of stoichiometry was studied by Santoro[27] and a maximum in hardness near the composition $TaC_{0.8}$ was found. A maximum was also observed in the present study at low stoichiometry but the decrease in hardness was associated with precipitation as shown in an electron micrograph, Figure 12. The lines shown do not appear to be slip lines but are thought to be due to the precipitation of either tantalum dicarbide or the zeta[19] phase. When hardness impressions were made closer to the normally observed Widmanstätten region (region of TaC + Ta_2C ppt. or zeta ppt.) the lines associated with the hardness impression fit the pattern in the Widmanstätten region thus indicating the lines are due to a precipitation phenomena which may be stress induced. Apparent maximums also occurred in the niobium-carbon and vanadium carbon systems and are assumed to be associated with the precipitation of a second phase.

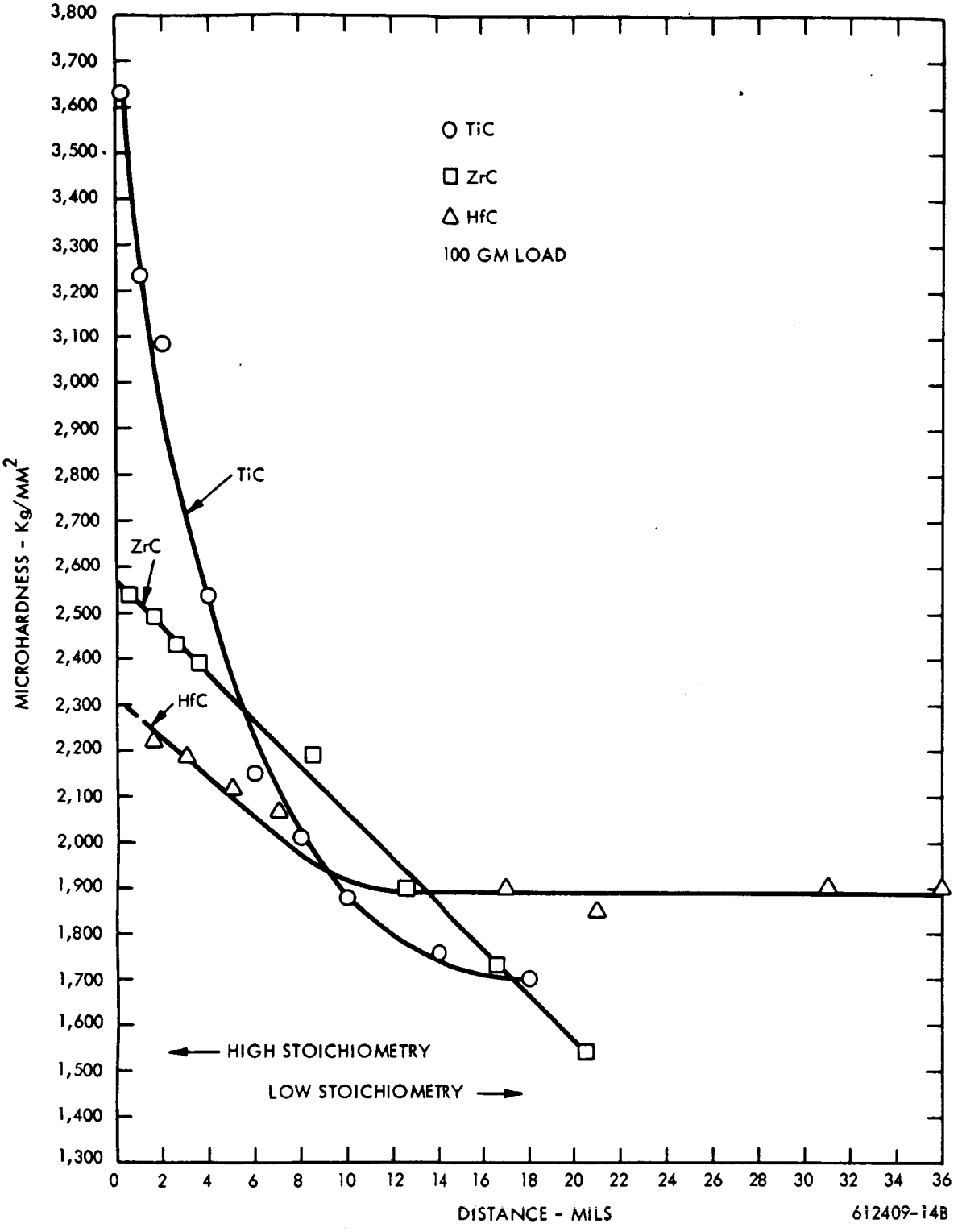

Figure 10. Microhardness of the Group IVB Carbides as a Function of Distance across the Width of the Carbide Scale (TiC-2300°C 144 minutes; ZrC-2800°C 27 minutes; HfC-3000°C 100 minutes.)

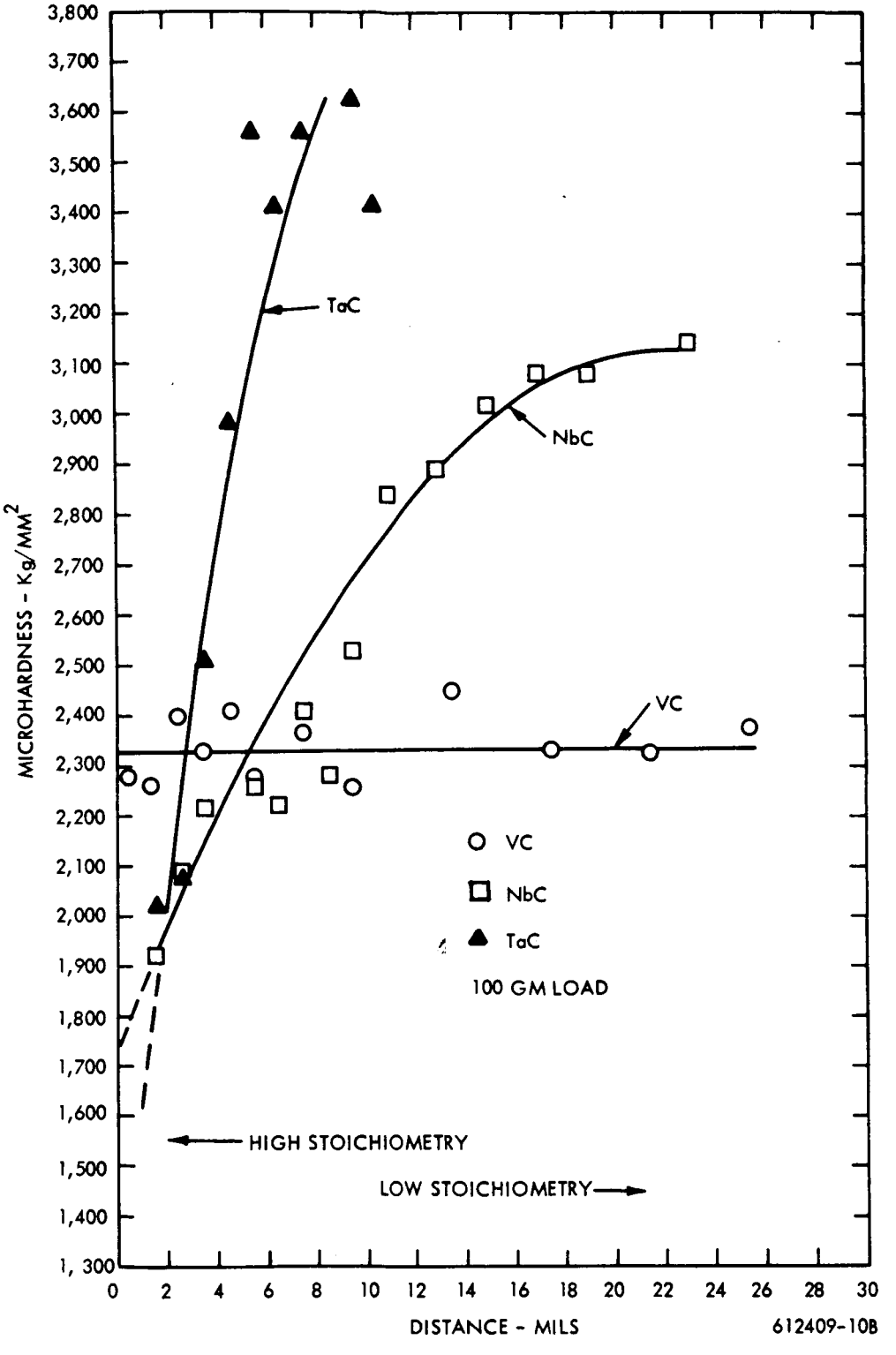

Figure 11. Microhardness of the Group VB Monocarbides as a Function of Distance across the Width of the Carbide Scale (VC-2300°C 144 minutes; NbC-2850°C 100 minutes; TaC-2600°C 5.5 hr.)

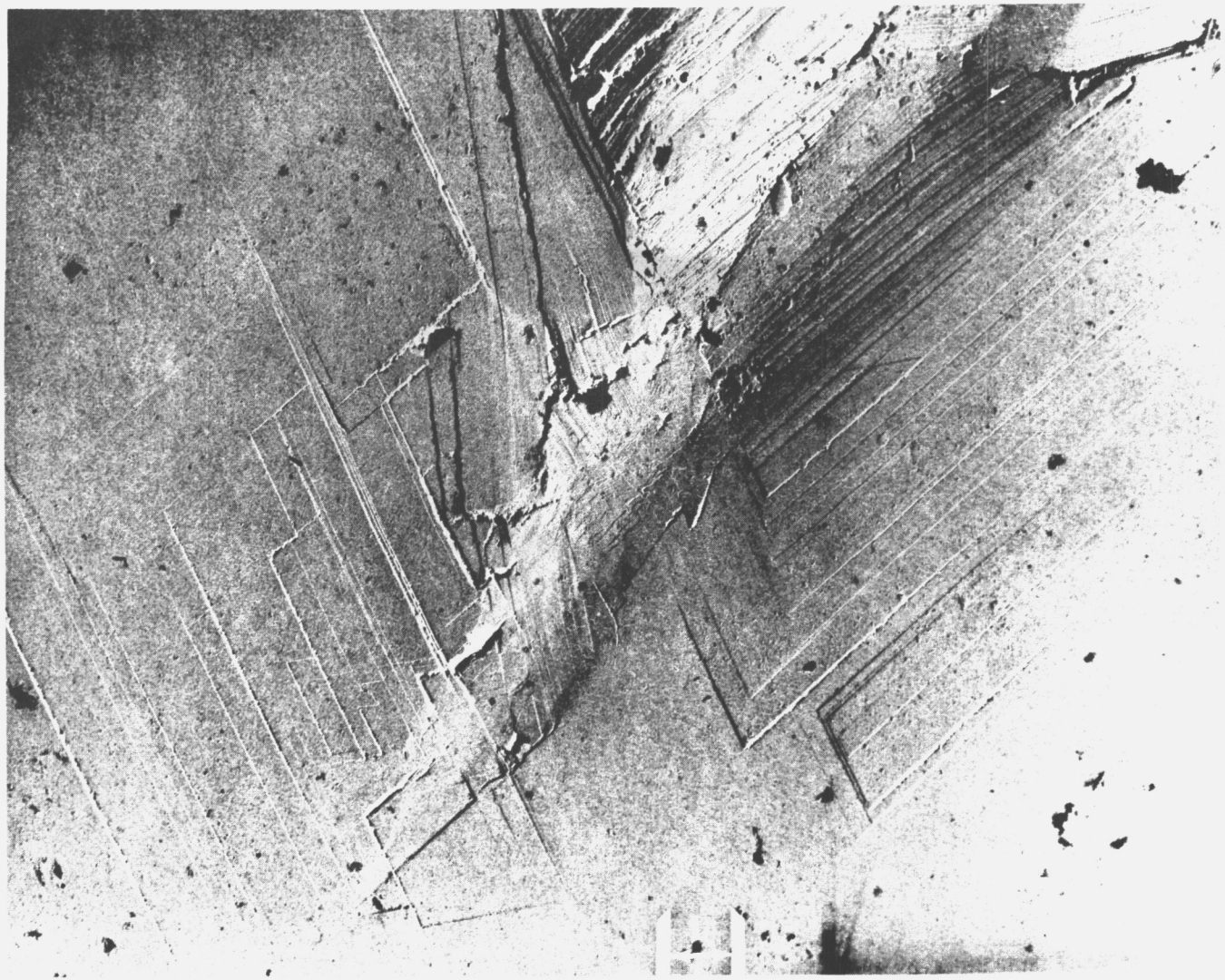

Figure 12. Electron Micrograph of Low Stoichiometry Tantalum Monocarbide Showing Precipitation Associated with the Hardness Impression. Load 500 grams.

3.4 YIELD STRESS

Specimens were mechanically tested in a radiantly heated Brew graphite resistance element furnace operated at one atmosphere of helium. A constant strain rate was applied with an Instron machine and the stress strain curve continuously recorded. Temperature measurements were made by sighting through a port in the graphite heater onto the surface of the sample with a Milletron two-color pyrometer previously calibrated against a standard tungsten filament lamp. Pyrolytic graphite end platens were used and strains were obtained from the crosshead movement.

The yield stress of the six monocarbides were determined at a strain rate of 0.02 per minute at 0.2 percent offset strain. The yield stress as a function of temperature is shown in Figures 13 and 14. Hafnium carbide has the highest yield stress at elevated temperatures while vanadium carbide has the lowest. The high yield stress of hafnium carbide however may be influenced by two factors not common to the other five monocarbides; 1) HfC contains approximately 1.5 percent zirconium and 2) the grain size is approximately a factor of three times smaller. The apparent discontinuity in the yield stress of zirconium carbide as a function of temperature appears real. There has been discussion[28] [29] as to whether a high temperature phase transformation exists (2000 to 2500°C) in zirconium carbide as evidenced by a sharp change in emissivity with temperature. High temperature x-ray studies are required to resolve this question.

The yield stress data was found to fit the expression $\sigma_{y.s.} = A \exp(-kT)$. The same type of relationship was given by Williams[30] for titanium carbide. A plot of log yield stress versus temperature for titanium carbide, vanadium carbide, and tantalum carbide is given in Figure 15. It is interesting to note that if the yield stress data can be extrapolated to lower temperatures it indicates that titanium carbide has a higher yield stress at room temperature than the other five carbides. Titanium carbide also exhibits the highest hardness at room temperature.

It was noted from the stress strain curves that strain hardening was greatest in tantalum carbide and decreased in the following order: NbC, HfC, ZrC, TiC and VC. The slope of the stress strain curve for tantalum carbide at ten percent strain varied from 60×10^3 to 45×10^3 psi per one percent strain over the temperature range of 2000 to 2700°C while vanadium carbide varied from 15×10^3 to 7×10^3 over the temperature range of 1700 to 2500°C.

The yield stress as a function of stoichiometry was investigated for tantalum carbide and titanium carbide to determine if the high temperature strength varies in the same manner as the room temperature hardness. Low stoichiometry test specimens were prepared by partial carburization of the rod, i. e., the diffusion anneal was terminated when only a few mils of metal remained. Thus uniform low stoichiometry samples were not obtained but samples of low stoichiometry when compared to high stoichiometry material should provide a preliminary indication as to how strength varies with composition. The yield stress and creep resistance of high and low stoichiometry titanium carbide are given in Figures 16 and 17. Both the yield stress and creep resistance are less in carbon deficient titanium carbide. This is in agreement with the yield stress data as a function of composition reported by Williams[30] and Hollox[16] and the hardness data reported in an earlier section of this report.

The yield stress and creep resistance of stoichiometric and substoichiometric tantalum carbide are shown in Figures 18 and 19. Like titanium carbide, the mechanical properties decrease with decreasing carbon content, this is in conflict with the lower temperature data of Steinitz[32] who reported that the creep resistance increased with decreasing stoichiometry and also with the hardness data reported earlier. The decrease in mechanical properties (>0.5 M. P.) as carbon is removed from the carbide can be understood if we assume deformation is diffusion controlled and that diffusion rates in the carbides are more dependent on the defect structure than on the bonding strength. It has been shown that both carbon diffusion[31] [33] [34] and metal diffusion[35] increase with decreasing stoichiometry as one would expect since the defect concentration is increased by the removal of carbon atoms. Thus, room temperature hardness varying with the bonding strength or Peierls force and high temperature properties varying with

the diffusivity is proposed to explain the observed behaviors. From Figures 18 and 19, it is apparent that as the temperature is lowered from 2500 to 2100°C the creep rate and the stress strain curves for $TaC_{1.0}$ and TaC_x become almost identical. In fact, the creep resistance of TaC_x is shown in Figure 19 to be greater than that for $TaC_{1.0}$ at 2100°C. It, therefore, appears that at approximately 2100°C ($\approx$0.5 M. P.) the mechanism controlling deformation is changing from diffusion controlled to a mechanism depending more on bonding strength. The increased creep resistance of tantalum carbide with decreasing stoichiometry determined by Steinitz[32] is consistent with a change in mechanism at approximately one half the melting point since his creep rate data was determined at less than one half the melting point. The mechanism controlling deformation in the carbides will be discussed in further detail in a later paper[36].

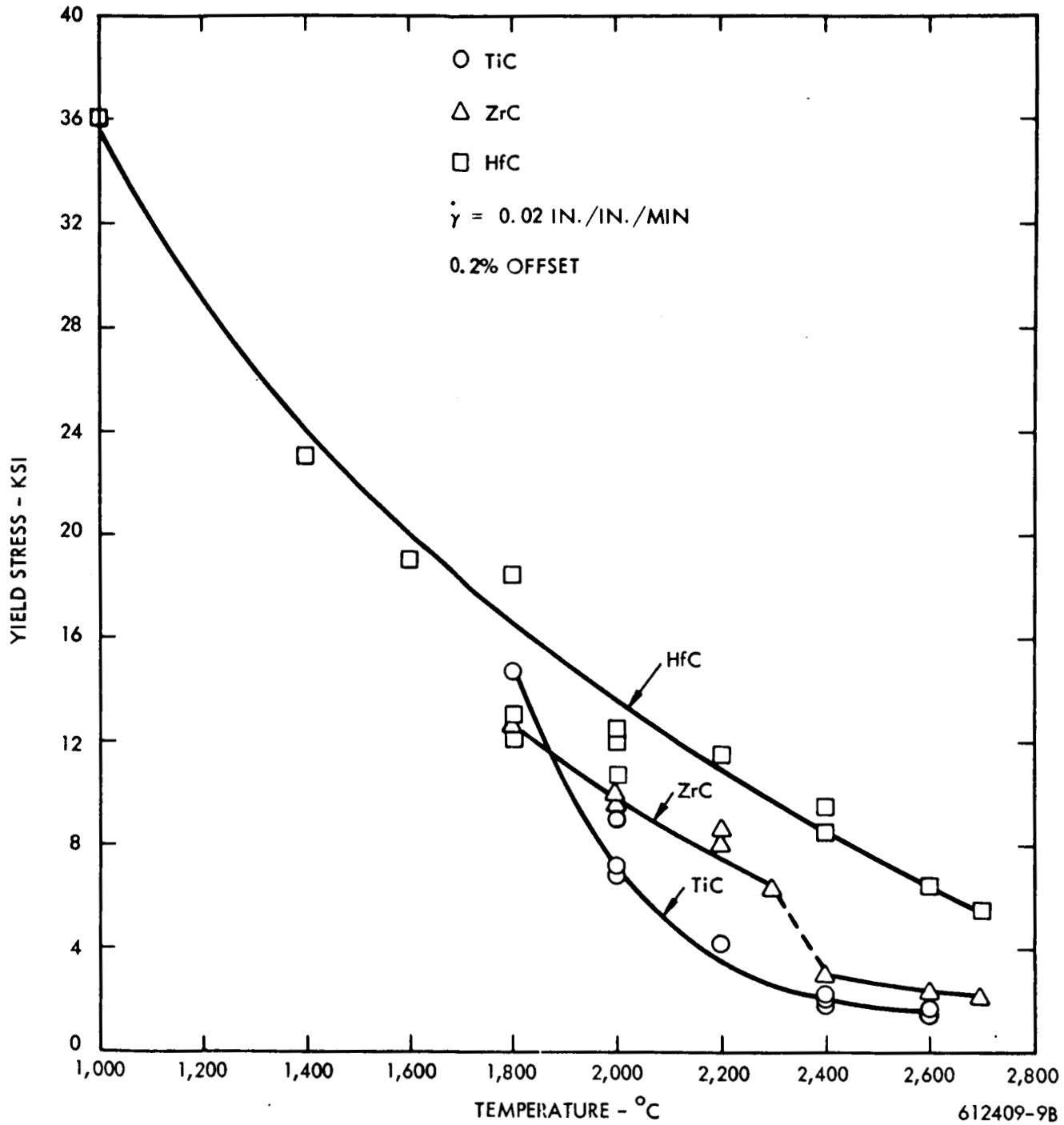

Figure 13. Yield Stress of the Group IVB Carbides as a Function of Temperature

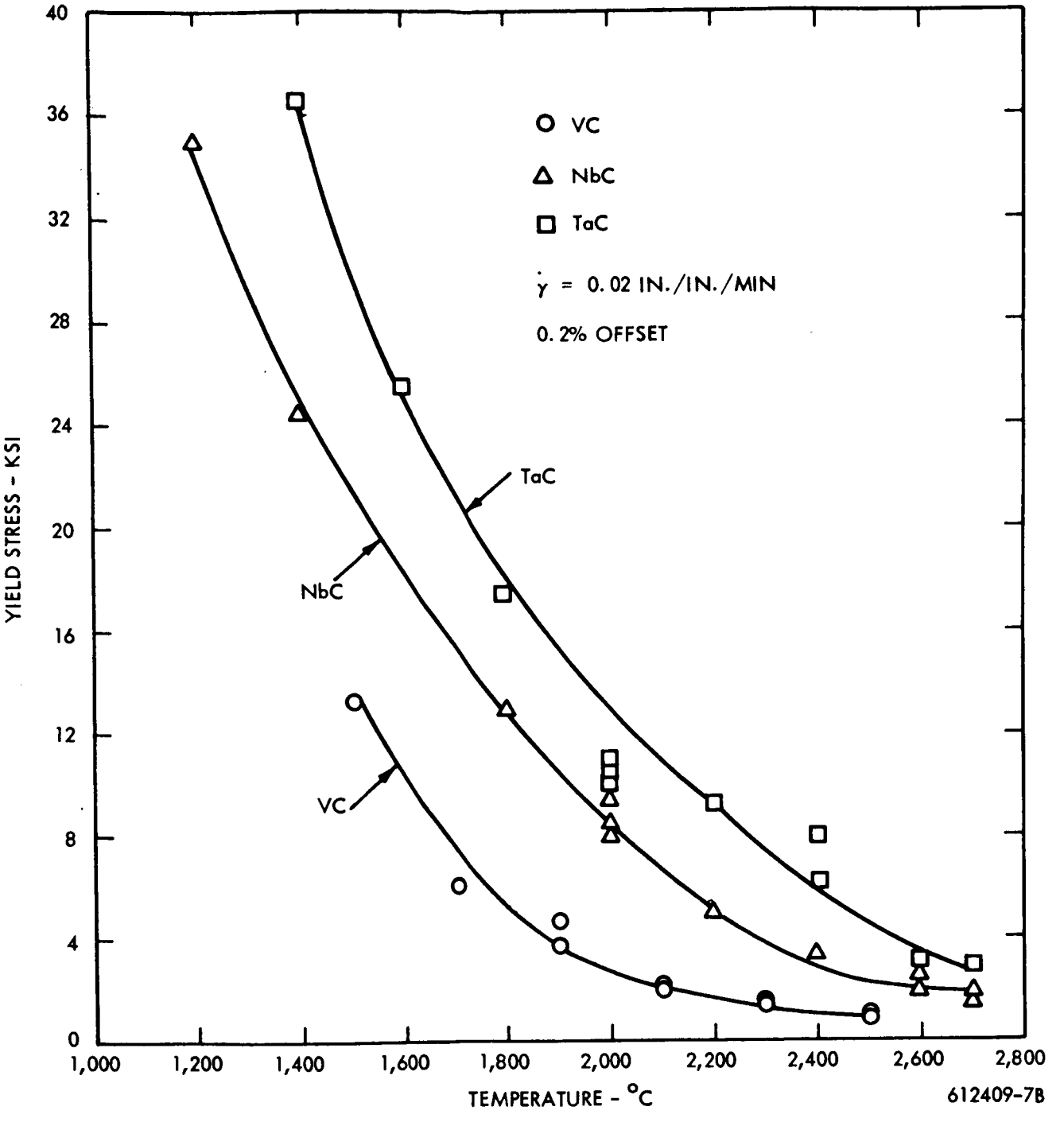

Figure 14. Yield Stress of the Group VB Monocarbides as a Function of Temperature

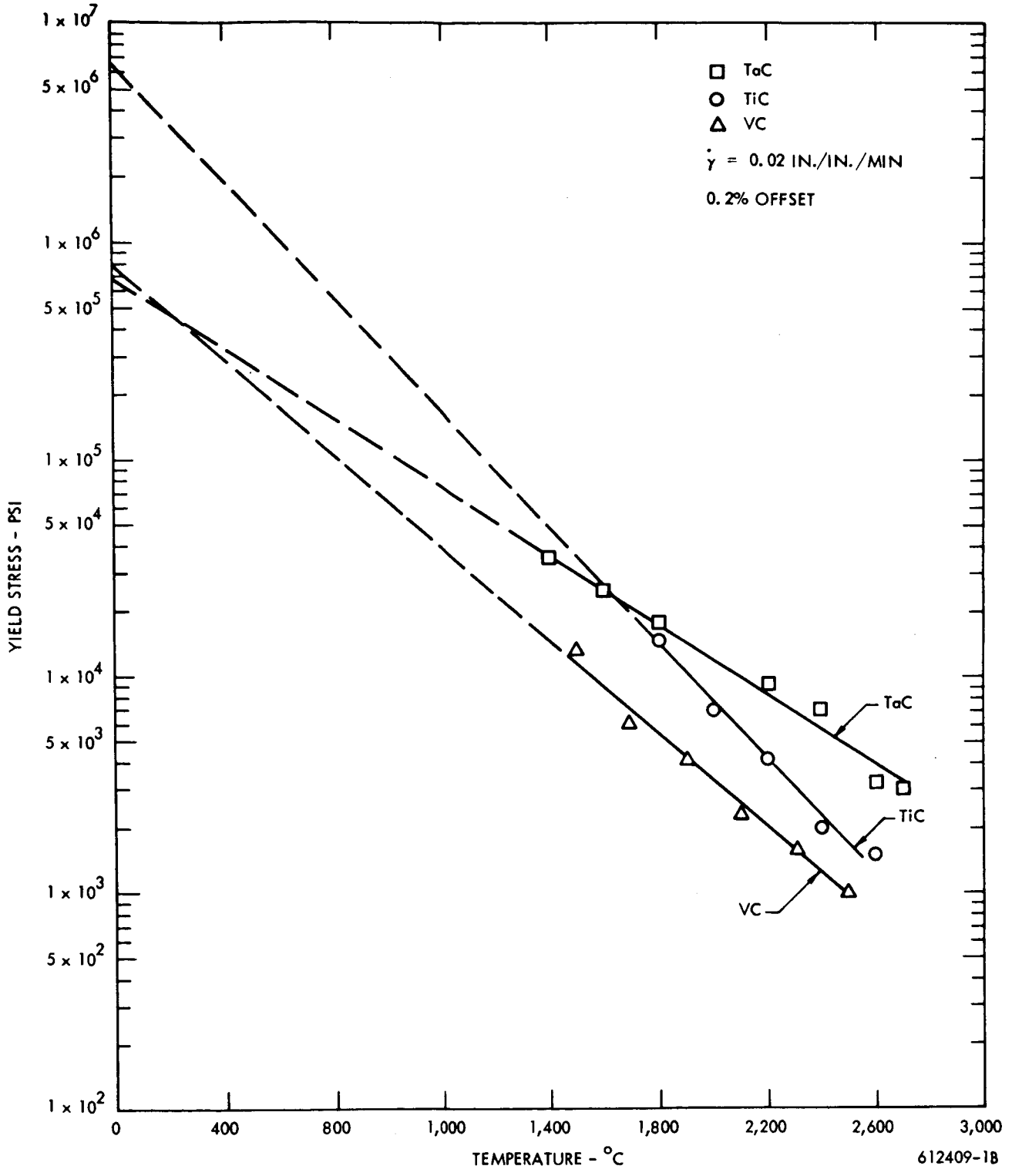

Figure 15. Log Yield Stress as a Function of Temperature

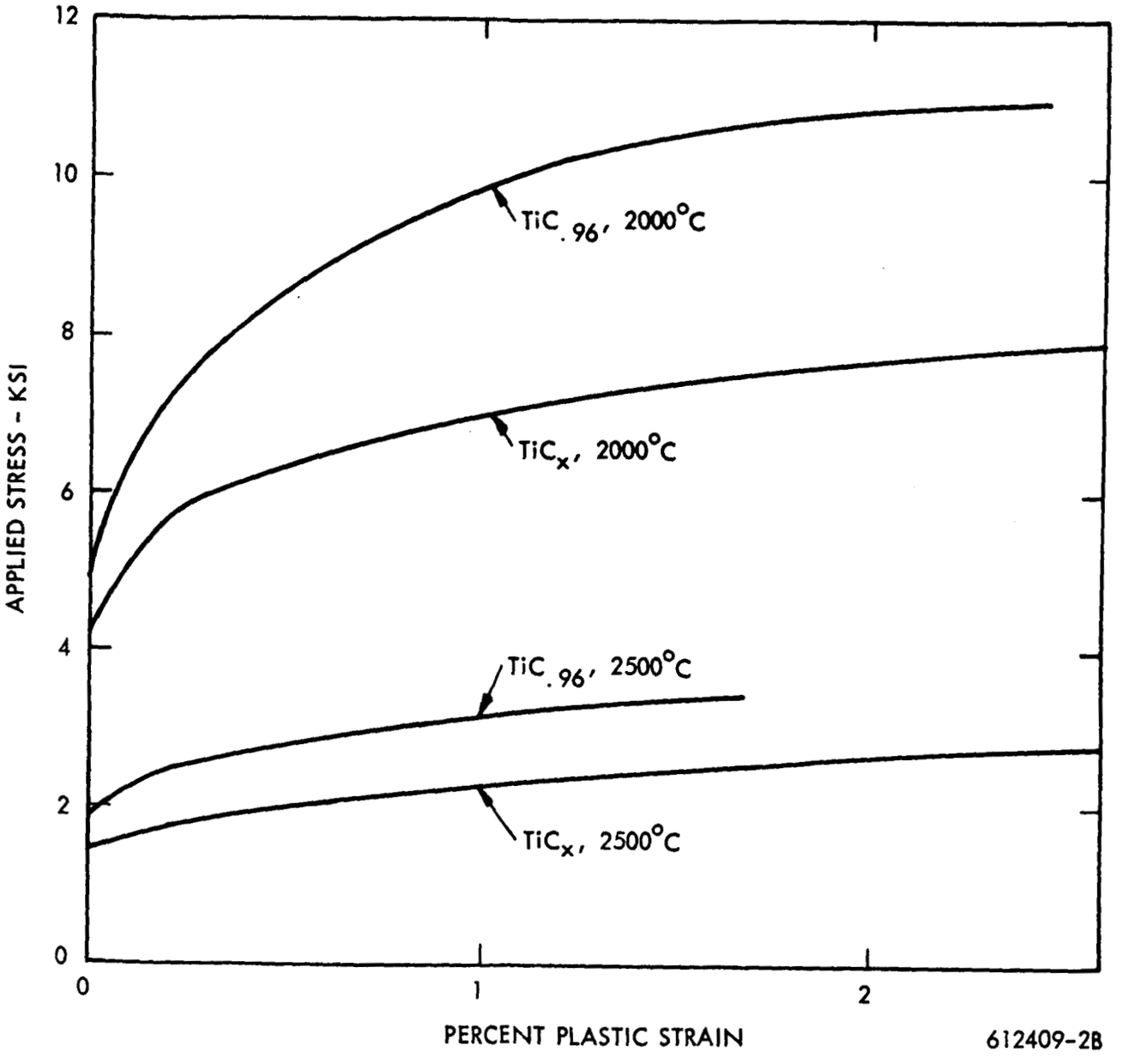

Figure 16. Stress Strain Curve for $TiC_{.96}$ and TiC_x. (1/4 inch diameter specimen, $0.02^{\cdot 96}$ min.$^{-1}$).

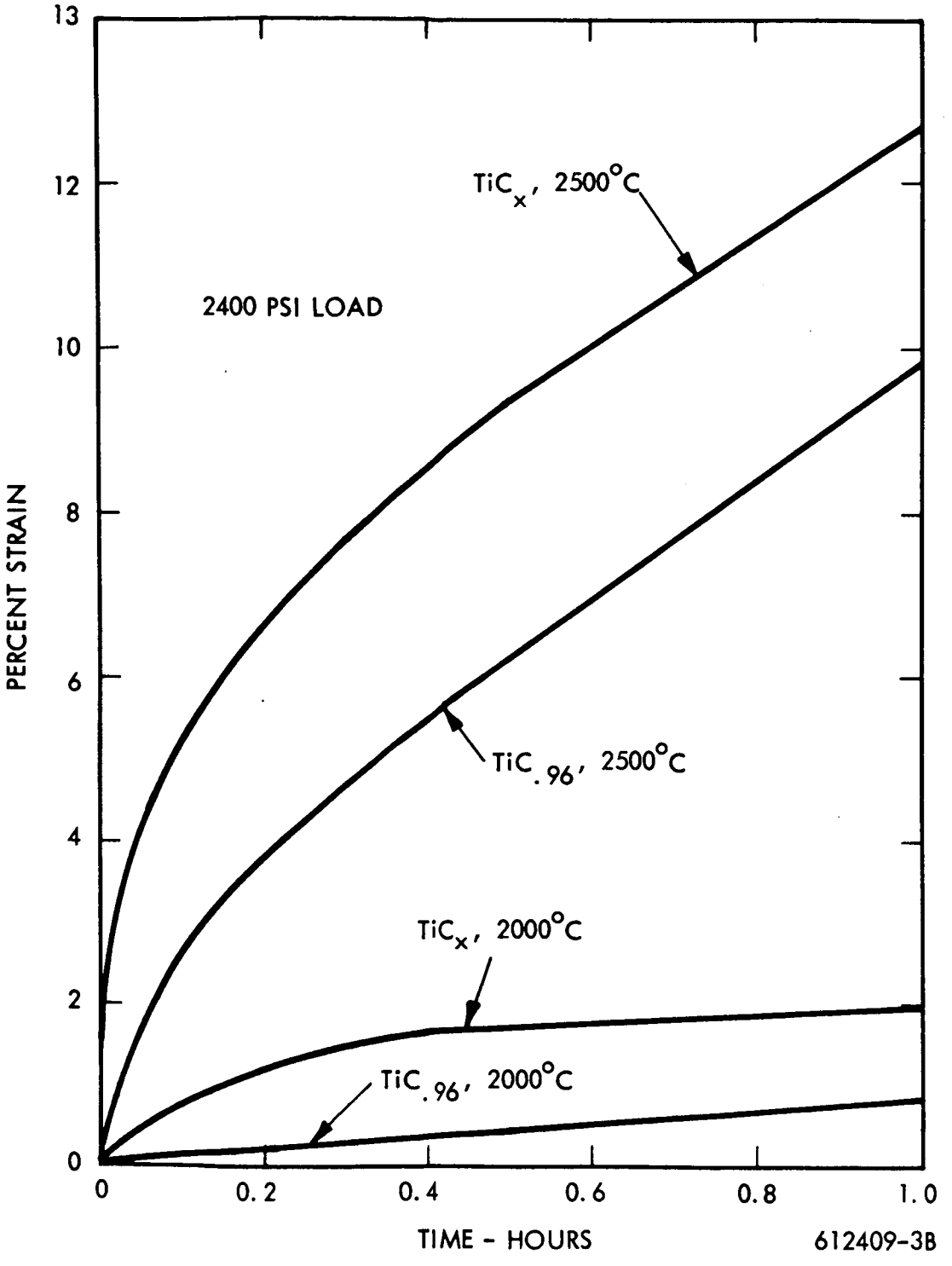

Figure 17. Creep of $TiC_{.96}$ and TiC_x. (1/4 inch diameter specimens)

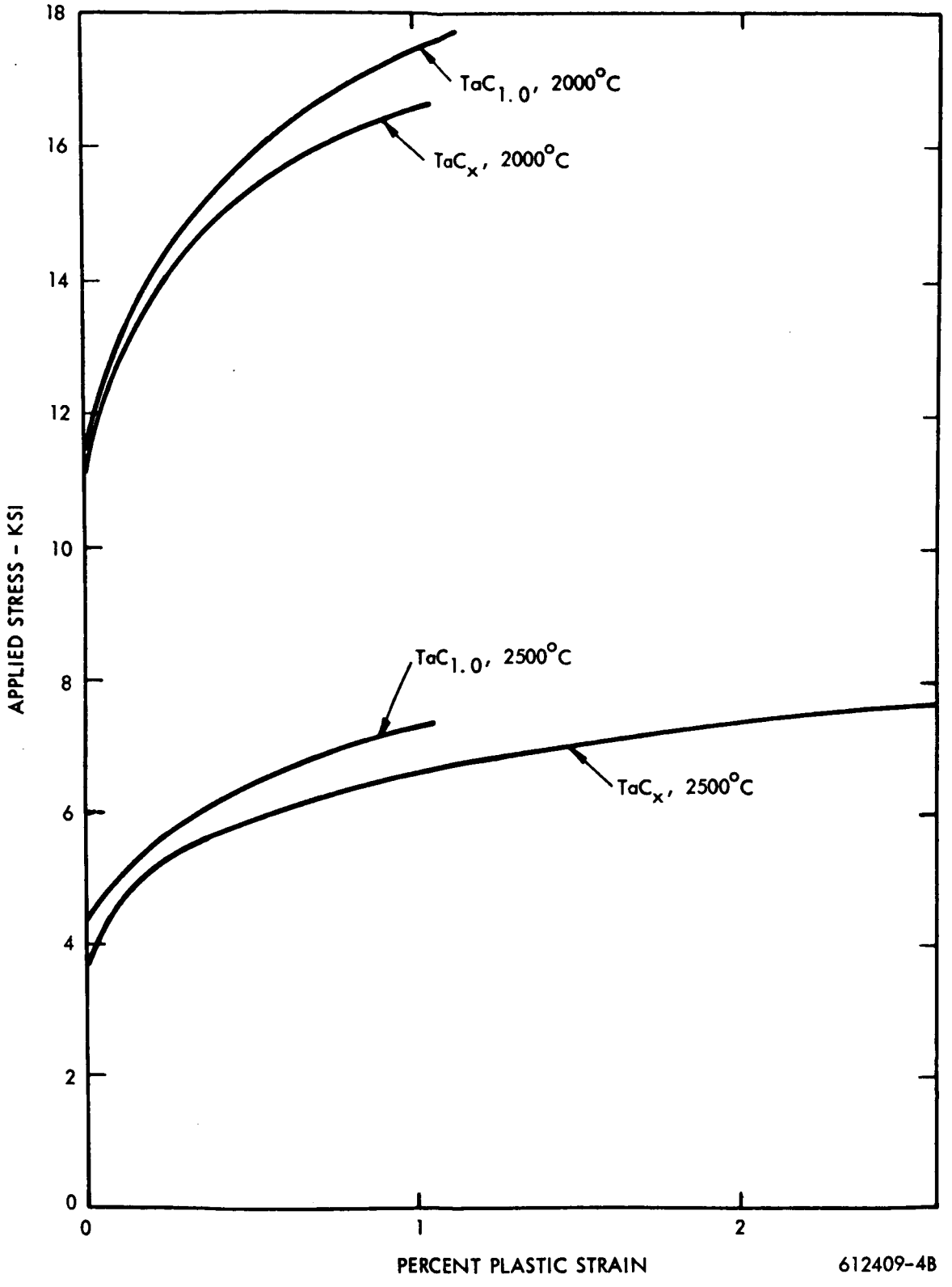

Figure 18. Stress Strain Curve for $TaC_{1.0}$ and TaC_x (1/4 inch diameter specimens 0.02 min^{-1})

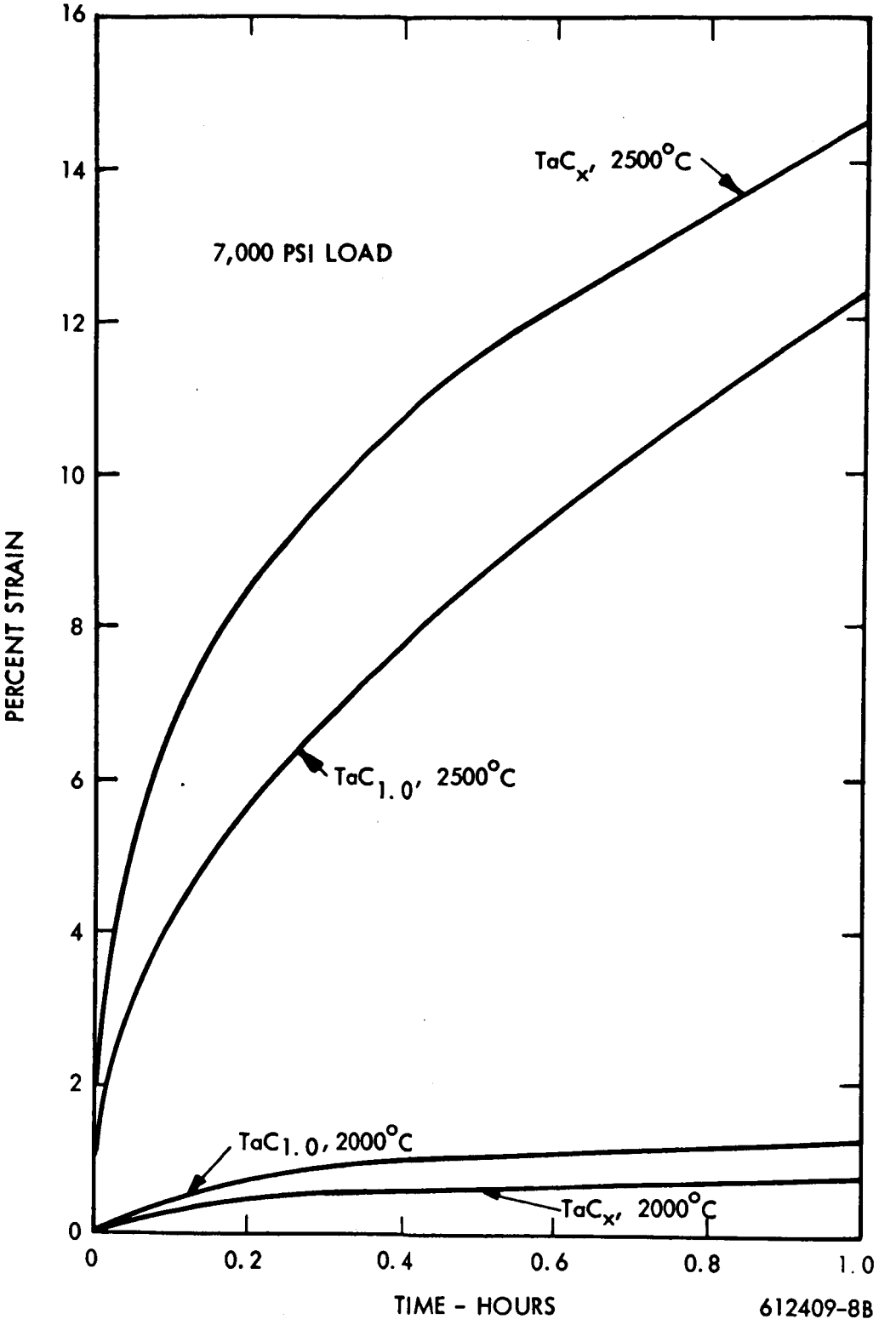

Figure 19. Creep of $TaC_{1.0}$ and TaC_x (1/4 inch diameter specimens)

3.5 GRAIN BOUNDARY SLIDING

Gross grain boundary sliding was observed in only two of the carbides studied; vanadium carbide and hafnium carbide. A photomicrograph of vanadium carbide and a photomicrograph of hafnium carbide are shown in Figures 20 and 21. Sliding became prevalent at approximately 1900°C for both carbides and increased with increasing temperature. Gross chemical analysis (Table 2) did not indicate an impurity content although grain boundaries were not analyzed per se. Due to time limitation a detailed study of grain boundary sliding was not possible.

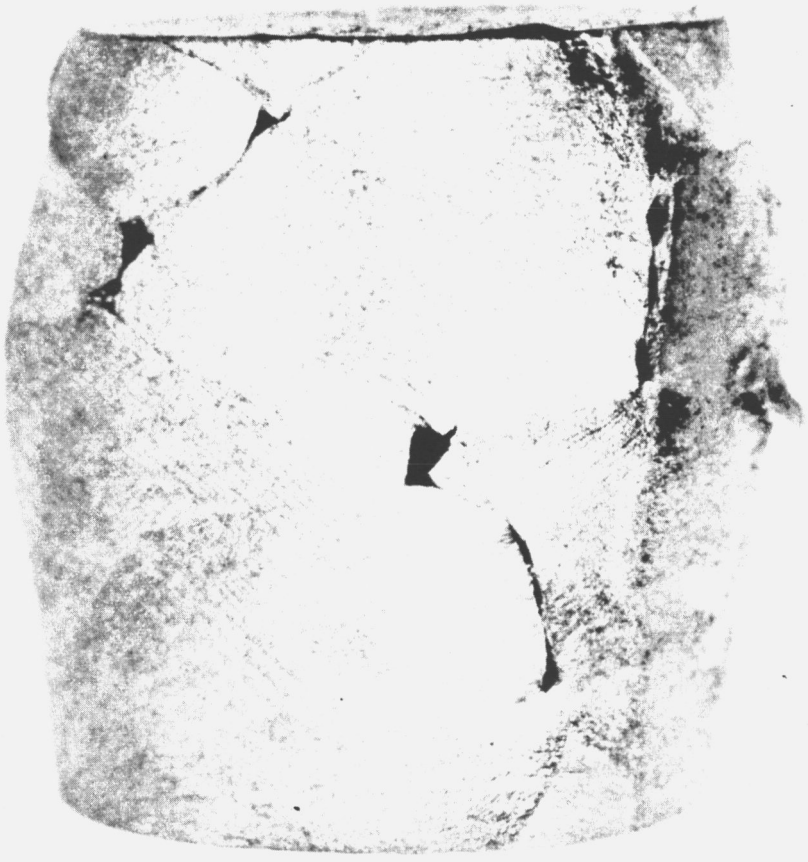

Figure 20. Photomacrograph of Vanadium Carbide Showing Gross Grain Boundary Sliding. Specimen Tested in Compressive Creep at 2300°C, 2000 psi for one hour giving 23 percent total strain. (3/8 inch diameter specimen)

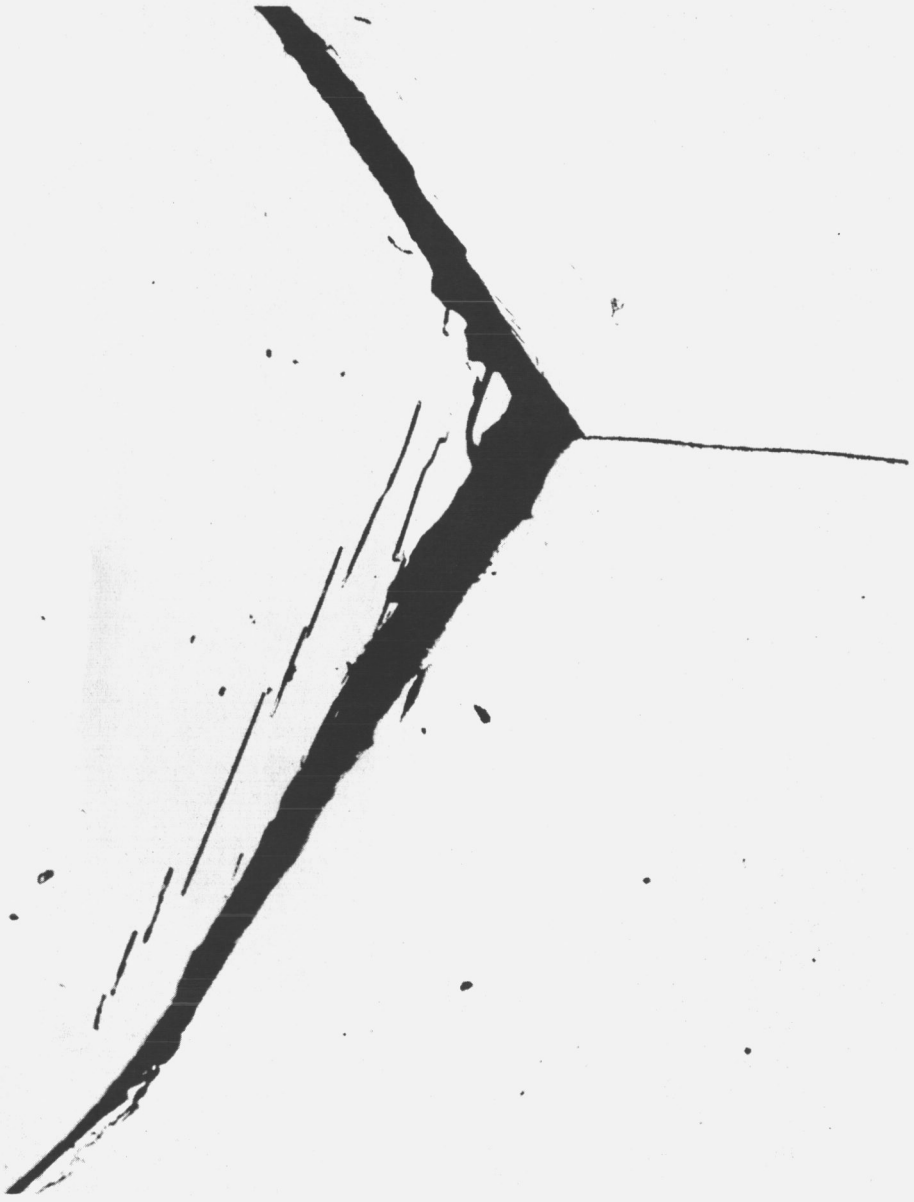

Figure 21. Photomicrograph of Hafnium Carbide Showing Grain Boundary Sliding. Sample Tested in Compression at 0.02 in/in/min, 2000°C to 8.3 percent Total Strain.

3.6 ACTIVATION ENERGY FOR DEFORMATION OF NIOBIUM MONOCARBIDE

If it is assumed that high temperature deformation is controlled by a thermally activated process, as is indicated by the strong temperature dependence of the yield stress with temperature, Figures 13 and 14, then it can be shown[37] that the energy required to overcome an energy barrier of height H* can be reduced by an applied resolved shear stress.

If we assume that a dislocation is held up at a barrier H* over a length L and the distance the dislocation must move to overcome the barrier is d, the activation volume V* may be defined as

$$V^* = Lbd \tag{1}$$

Where b is the Burgers vector.

Assuming that the applied shear stress can assist in overcoming the barrier H* the apparent activation energy can be given by

$$\Delta Q = H^* - V^* \tau^* \tag{2}$$

where

$$\tau^* = \tau_a - \tau_i \tag{3}$$

τ_a = applied shear stress

τ_i = long range internal stress

τ_i was determined from Figure 14 and taken to be the value at which the yield stress becomes athermal.

The above parameters are defined in the force distance diagram[38] given in Figure 22. The general equation for strain rate is

$$\dot{\gamma} = K \exp\left(-\frac{\Delta Q}{kT}\right) \tag{4}$$

where

$$K = NAb\vartheta \tag{5}$$

N = number of pieces of dislocation likely to slip at any moment

A = area swept out by a dislocation when it slips

ϑ = frequency of vibration of the dislocation

Differentiating equation (4)

$$\Delta Q = kT^2 \left(\frac{\delta \ln \dot{\gamma}}{\delta T}\right)_{\tau^*} \tag{6}$$

and separating variables

$$\Delta Q = -kT^2 \left(\frac{\delta \ln \dot{\gamma}}{\delta \tau^*}\right)_T \left(\frac{\delta \tau^*}{\delta T}\right)_{\dot{\gamma}} \tag{7}$$

The value of ΔQ can thus be determined if the terms $\left(\frac{\delta \ln \dot{\gamma}}{\delta \tau^*}\right)_T$ and $\left(\frac{\delta \tau^*}{\delta T}\right)_{\dot{\gamma}}$ are evaluated as shown below.

The shear stress was assumed to be one half the applied stress and the term $\left(\frac{\delta \tau^*}{\delta T}\right)_{\dot{\gamma}}$ was determined from Figure 14 as one half the slope at 2100°C. The change in yield stress determined at different strain rates at 2100°C is given in Figure 23 and thus the term $\left(\frac{\delta \ln \dot{\gamma}}{\delta \tau^*}\right)_T$ was evaluated. Thus, from equation 7 a value of 118.5 K cal/mole was obtained. ΔQ however is only the apparent activation energy ($\Delta Q = H^* - V^* \tau^*$).

The activation volume in the term $V^* \tau^*$ can be evaluated by combining equations 2 and 4.

$$\dot{\gamma} = K \exp - \left(\frac{H^* - V^* \tau^*}{kT}\right) \tag{8}$$

taking the derivative

$$V^* = kT \left(\frac{\delta \ln \dot{\gamma}}{\delta \tau^*}\right)_T \quad (9)$$

and multiplying equation 9 by τ^*

$$V^* \tau^* = kT \left(\frac{\delta \ln \dot{\gamma}}{\delta \ln \tau^*}\right)_T \quad (10)$$

The term $\left(\frac{\delta \ln \dot{\gamma}}{\delta \ln \tau^*}\right)_T$ can be determined from the slope of Figure 24 at $\tau^* = 2,300$ psi corresponding to the yield stress at 2100°C and thus giving a value of $V^* \tau^*$ equal to 14.5 K cal/mole. Thus the true activation energy H* from equation 2 is $H^* = \Delta Q + V^* \tau^* = 118.5$ kcal/mole + 14.5 K cal/mole = 133 K cal/mole. This is in good agreement with the calculated value for diffusion of niobium in niobium carbide, $(H^*)^{Nb}_{NbC}$ = 130 to 165 K cal/mole calculated by Cadoff[35] or by multiplying the melting point by 38 giving an activation energy of 136 K cal/mole. The activation energy for carbon diffusion in niobium carbide was determined[31] to be 88 K cal/mole.

The strain rate dependence of the stress can be given by[39]

$$\dot{\gamma} = B (\tau^*)^m \quad (11)$$

Differentiating equation (11),

$$m = \frac{\delta \ln \dot{\gamma}}{\delta \ln \tau^*} \quad (12)$$

From the slope of Figure 24 a value of m equal to 3.1 was obtained at 2100°C and is in the normal range observed[40] for covalent solids.

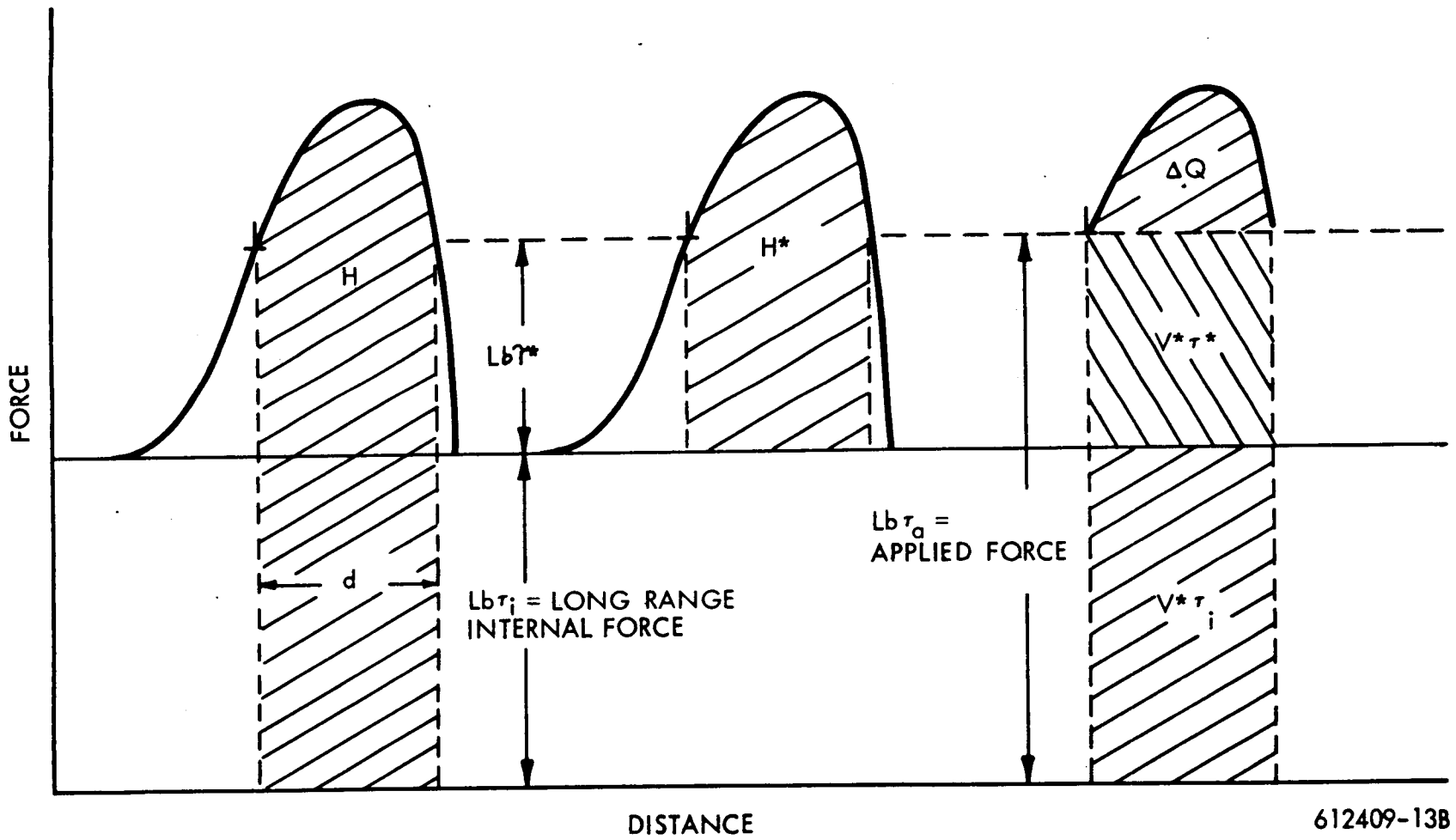

Figure 22. Force Acting on a Dislocation as a Function of Lattice Position

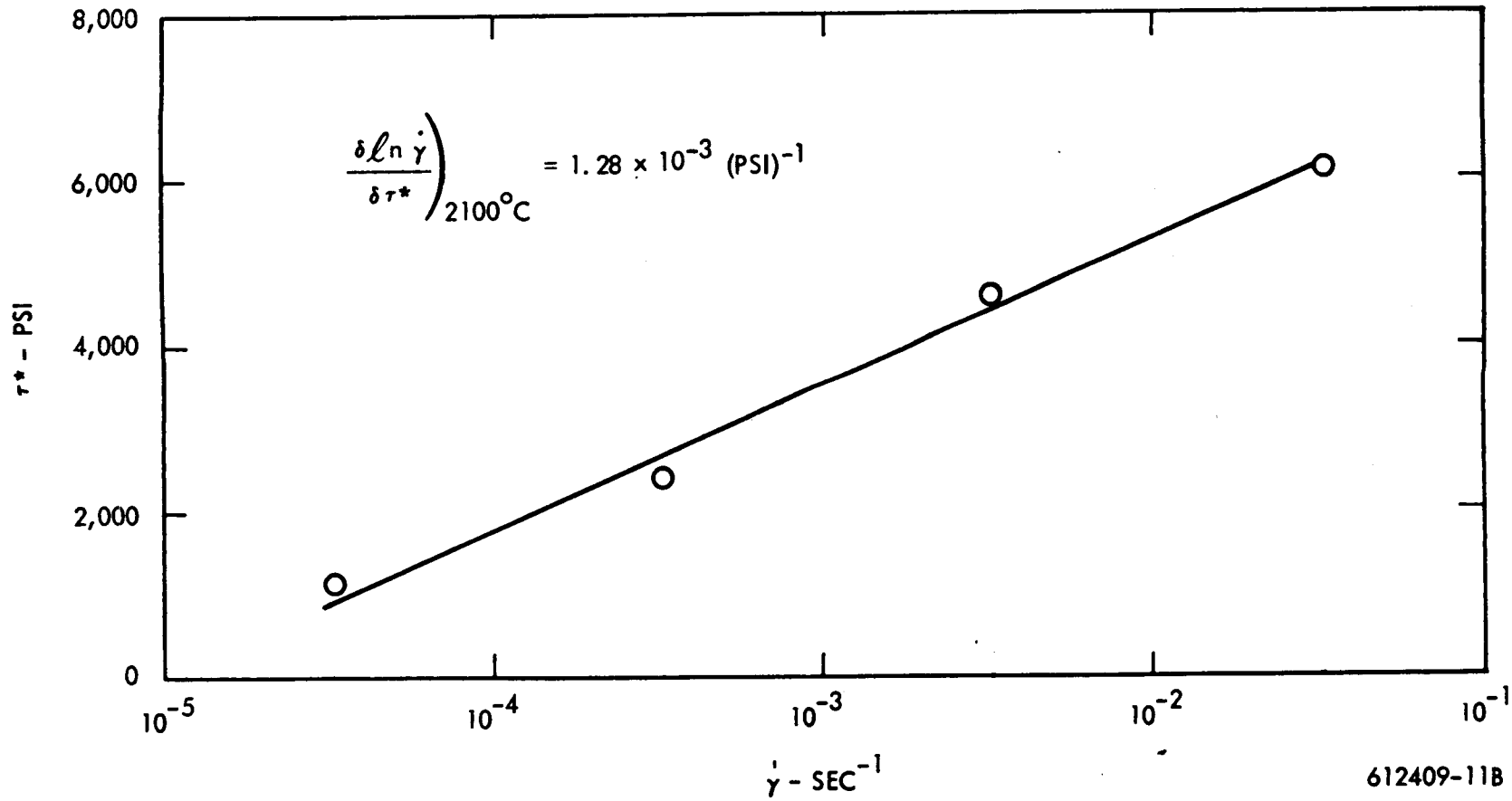

Figure 23. τ^* Versus Log of the Applied Strain Rate

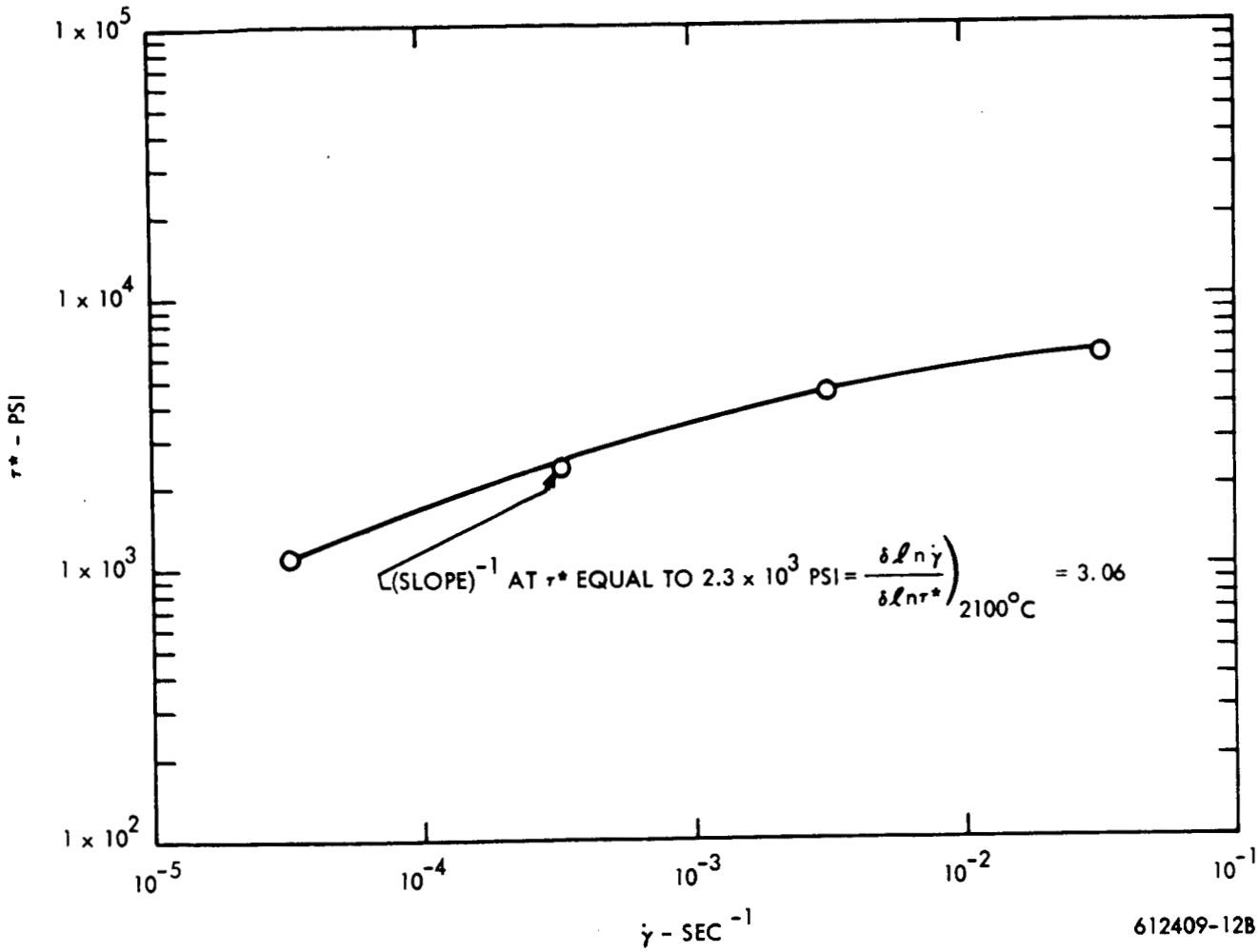

Figure 24. In τ * Versus Log of the Applied Strain Rate

4.0 CONCLUSIONS

It has been shown that samples made by liquid state carburization are of high purity and are suitable for mechanical property studies of the Group IVB and VB monocarbides. It was proposed that the room temperature hardness of the carbides as a function of stoichiometry is probably related to a high Peierls force, while at temperatures greater than one half the melting point the mechanical properties are related to metal diffusion. For high temperature applications solid solution alloy carbides appear interesting if the diffusion rates can be decreased by 1) increased bonding strength and 2) decreased defect concentration.

5.0 ACKNOWLEDGEMENTS

The author expresses his appreciation to Dr. E. I. Salkovitz, Chairman of the Department of Metallurgical and Materials Engineering, who was his M. S. thesis advisor, to L. L. France, his supervisor, to E. F. Vandergrift who performed the mechanical testing, and to P. S. Gaal who conducted the thermal expansion measurements.

6.0 REFERENCES

1. L. M. Adelsburg, and L. H. Cadoff; Trans. AIME, 239, (1967) 933.
2. E. Rudy, C. P. Harmon, C. E. Brukl, Report AFML-TR-62-2, Part 1, Vol. 2, 1965.
3. L. M. Adelsberg, L. H. Cadoff, and J. M. Tobin, Trans. AIME 972 (1966), 236.
4. R. V. Sara, C. E. Lowell, and R. T. Dolloff, J. Am. Cer. Soc., 48 (1965) 243.
5. R. V. Sara, Trans. Met. Soc. AIME, 233, (1965) 1683
6. L. M. Adelsberg and L. H. Cadoff - J. Am. Cer. Soc., 51, (1968) 213.
7. E. K. Storms and R. J. McNeal, J. Phy. Chem. 66, (1962) 1401
8. E. K. Storms and N. H. Krikorian, J. Phy. Chem., 64, (1960) 1471
9. W. F. Brizes and J. M. Tobin, J. Am. Cer. Soc., 50, (1967) 115
10. E. Rudy and D. P. Harmon, Report No. AFML-TR-65-2 Part 1, Vol. V.
11. R. G. Lye and E. M. Logothetis, Phy. Rev. 147, (1966) 622
12. W. S. Williams, Phys. Rev. 135, (1964) 505
13. J. Piper, Powder Met. 29 (1958).
14. R. G. Lye, "Atomic and Electronic Structure of Metals", ASM Seminar, Oct. 1966.
15. W. S. Williams and R. D. Schaal, J. Appl. Phy., 33, (1962) 955.
16. G. E. Hollox and R. E. Smallman, J. Appl. Phy., 37 (1966) 818.
17. E. Ryshkewitch, J. Am. Cer., 36, (1953) 65.
18. P. Gaal. To be published.
19. Metals Handbook, Vol. 1, 8 ed., 1961.
20. R. J. Fries and L. A. Wahman, J. Am. Cer. 50 (1967) 475.

REFERENCES (CONTINUED)

21. W. F. Brizes, to be published.

22. Schwarzkopf and Kieffer, Refractory Hard Metals , N. Y., MacMillan Co., 1953.

23. Samsonov and Umanskiy, "Hard Compounds of Refractory Metals", Technical Translation NASA-TTF-102.

24. W. S. Williams and R. G. Lye Union Carbide Corp., ML-TDR-64-25, Part II, 1965.

25. L. H. Cadoff and W. F. Brizes, to be published.

26. G. Jangg, R. Kieffer and L. Usner, J. Less - Common Metals 14 (1968) 269.

27. G. Santoro, Trans. AIME 227 (1963) 1361.

28. P. T. Shaffer, J. Am. Cer. Soc. 46 (1963) 177.

29. L. N. Grossman, J. Am. Cer. Soc. 48 (1965) 236.

30. W. S. Williams, J. Appl. Phy. 35 (1964) 1329.

31. W. F. Brizes, L. H. Cadoff, and J. M. Tobin J. Nuc. Mat. 20 (1966) 57.

32. R. Steinitz Conference on Applications of Nonfissionable Ceramics, Washington, D. C., May, 1966, Sponsored by Am. Nuc. Soc. and Am. Cer. Soc.

33. R. Resnick and L. Seigle, Trans. AIME 236 (1966) 1732.

34. W. F. Brizes, to be published J. Nuc. Mat., May 1968.

35. L. H. Cadoff, WANL-TME-1760.

36. W. F. Brizes, to be published, Deformation of the Group IVB and VB Transition Metal Carbides.

37. H. Conrad and S. Frederick, Acta Met. 10 (1962) 1013.

38. D. P. Gregory, Acta Met. 11 (1963) 455.

39. J. C. M. Li, Canadian J. Phy. 45 (1967) 493.

40. A. R. Chaudhuri, J. R. Patel and L. G. Rubin, J. Applied Physics, 33 No. 9, September 1962, p. 2736.